

New constraints on the timing of gold formation in the Sierra Foothills province, central California

Erin E. Marsh

U.S. Geological Survey, Box 25046, Mail Stop 973, Denver Federal Center, Denver, CO, 80225-0046, USA

Richard J. Goldfarb

U.S. Geological Survey, Box 25046, Mail Stop 973, Denver Federal Center, Denver, CO, 80225-0046, USA

and

*School of Earth and Geographical Sciences (M004), The University of Western Australia,
Crawley, WA, 6009, Australia*

Michael J. Kunk

U.S. Geological Survey, 12201 Sunrise Valley Drive, Reston, VA, 20192, USA

David I. Groves

*Centre for Exploration Targeting (M006), The University of Western Australia,
Crawley, WA, 6009, Australia*

Frank P. Bierlein

*Centre for Exploration Targeting (M006), The University of Western Australia,
Crawley, WA, 6009, Australia, and
AREVA NC Australia Ltd., 80 Leader Street, Forestville, SA, 5035, Australia*

Robert A. Creaser

Department of Earth and Atmospheric Sciences, University of Alberta, Edmonton, Alberta, Canada

ABSTRACT

Gold-related alteration and sulfide minerals were collected from deposits and occurrences throughout the Sierra foothills gold province to constrain timing of the ore formation relative to the geologic evolution of the southernmost part of the Cordilleran orogen. Argon-argon isotope ($^{40}\text{Ar}/^{39}\text{Ar}$) dating of mariposite from six gold deposits within the highly productive Mother Lode gold belt along the Melones fault zone constrains ore deposition to ca. 134-128 Ma. Micas from deposits along the Bear Mountain fault system to the west and within the East Gold belt to the east are slightly younger at ca. 128-125 Ma. Gold formation continued until about 115 Ma, as is recorded at the Pine Tree/Josephine deposit at the southern end of the Melones fault system and in the Alleghany and Downieville districts in the northern part of the Sierra foothills goldfields. Attempts at Re-Os isotope dating of gold-related pyrite and

e-mail: Marsh: emarsh@usgs.gov; Goldfarb: goldfarb@usgs.gov; Kunk: mkunk@usgs.gov; Groves: dgroves@segs.uwa.edu.au; Bierlein: frank.bierlein@afmex.com.au; Creaser: robert.creaser@ualberta.ca

Marsh, E.E., Goldfarb, R.J., Kunk, M.J., Groves, D.I., Bierlein, F.P., and Creaser, R.A., 2008, New constraints on the timing of gold formation in the Sierra Foothills province, central California, *in* Spencer, J.E., and Titley, S.R., eds., Ores and orogenesis: Circum-Pacific tectonics, geologic evolution, and ore deposits: Arizona Geological Society Digest 22, p. 369-388.

arsenopyrite from the Grass Valley district, as well as at many other deposits within the Sierra Nevada foothills, were unsuccessful because of the generally low rhenium concentrations of the sulfide minerals within the goldfields. The new argon-argon data constrain much of the gold formation in the Sierra foothills to a 20-m.y.-long period in the Early Cretaceous that correlates with major changes in Melones/Bear Mountain fault kinematics and Pacific basin plate motions. In contrast, older Late Jurassic gold events in the Grass Valley district likely relate to westward extrusion of the Klamath Mountains block from the Sierra foothills.

INTRODUCTION

High-grade quartz veins of the Sierra foothills gold province have yielded about 40 Moz Au (Moz = million ounces), yet the timing of mineralization remains poorly defined, particularly in relationship to the region's geologic history. The gold deposits are mainly located adjacent to the Bear Mountain and Melones fault systems and their northerly equivalents, and are within medium- to high-grade metasedimentary and metavolcanic rocks (Fig. 1). Evidence of synkinematic gold veining has been observed in several of the main deposits, but most observations indicate that veining occurred after Late Jurassic regional metamorphism. Although there are a few K-Ar and Rb-Sr dates reported in the literature for specific deposits in the gold province, the data set lacks robustness and minor inconsistencies in the data have hindered understanding of the ultimate ore-controlling processes. In an effort to clearly define the timing of gold deposition, hydrothermal mineral phases from many of the gold deposits along the length of the entire foothills province were collected for analyses using precise geochronological methods.

Tectonic setting

The Cordilleran miogeocline of western North America was a dominant feature throughout the Paleozoic. Between the end of the Proterozoic and Early Devonian, the continental margin of western North America experienced growth by addition of westerly-thickening shelf and slope strata (Poole et al., 1993). Obduction of oceanic rocks onto the Cordilleran margin occurred during the Late Devonian-Early Carboniferous Antler and the Permian-Triassic Sonoma events. The latter event was coupled with initial accretion of near-shore oceanic arcs to form the more landward parts of the present-day Sierra foothills and Klamath Mountains physiographic provinces (Dickinson, 2004, 2008).

Several major tectonic events associated with Cordilleran orogenesis are recognized to have occurred during Mesozoic evolution of the Sierra foothills (Fig. 2; Goldfarb et al., 2008).

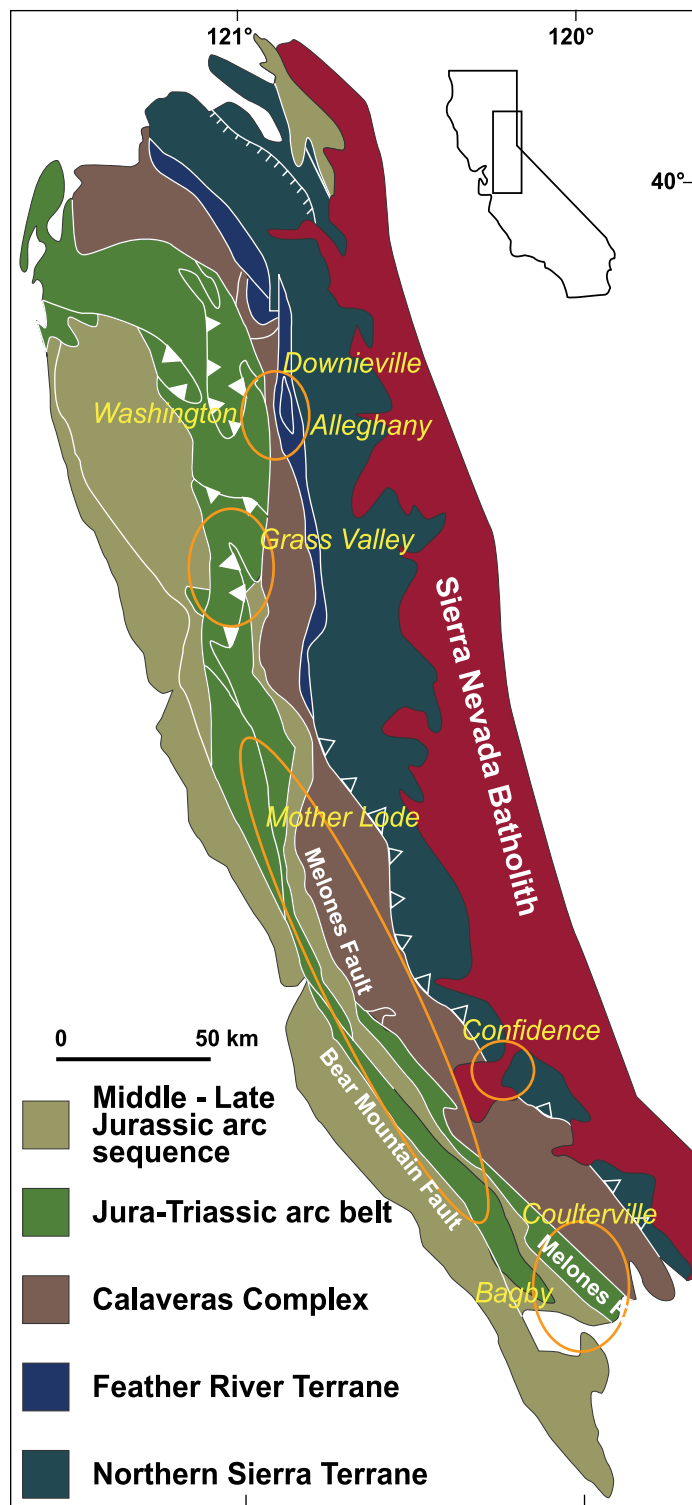


Figure 1. Terrane map of the western Sierra Nevada Foothills metamorphic belt with location of gold districts from which this study's samples were taken. Modified from Snow and Scherer (2006).

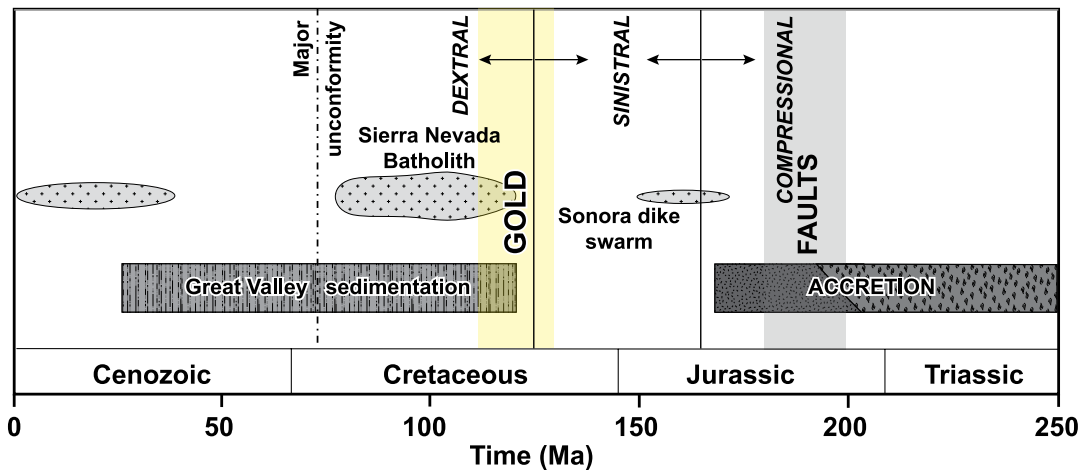


Figure 2. Schematic diagram of major regional tectonic events in the Sierra Nevada Foothills metamorphic belt.

From 272–166 Ma, the terranes of the foothills province were accreted to the continental margin (Sharp, 1988; Standlee, 1978). The terranes hosting the gold deposits are dominated by mafic to intermediate volcanoclastic rocks, mélangé, and flysch. West-vergent thrust faulting along terrane suture zones was the focus of deformation between 197 and 177 Ma within the Jura-Triassic arc belt of Snow and Scherer (2006), which consists of the Foothills Ophiolite and Sullivan Creek terranes of previous workers and represents the westernmost group of exposed terranes in the foothills. This thrusting is probably associated with the main accretionary event of the terranes along the western side of earlier docked terranes. These major fault systems have been shown to dip steeply beneath the western side of the Sierra batholith (Landefeld, 1988). During the Late Jurassic, when terrane accretion stepped seaward of the foothills terranes, geotherms may have begun to rise along these fault boundaries (Landefeld, 1988). Post-accretionary magmatism is represented by terrane-stitching plutons that young from ca. 170–160 Ma along the eastern margin of the amalgamated terranes to ca. 140 Ma along the margins of the westernmost terranes (Dickinson, 2008).

From about 145–124 Ma, the region experienced sinistral strike-slip movement, mainly along the reactivated thrust fault systems, which shifted to dextral strike-slip at ~125 Ma (Glazner, 1991; Umhoefer, 2003). This was also the time of development of regional cleavage and lower greenschist to lower amphibolite grade metamorphism (e.g., Saleeby et al., 1989). The Sierra batholith was intruded from 125–80 Ma between the accreted oceanic lithosphere to the west and North American Proterozoic lithosphere to the east (Glazner, 1991), with the most voluminous magmatism at 100–84 Ma (Saleeby et al., 2003). Throughout the Early Cretaceous and into the Late Cretaceous, both plutonism and deformation have been noted to move eastward; transpressive strike-slip along the Sierra batholith crest and eastern margins occurred as recently as ca. 80 Ma (Tobisch et al., 1995; Horsman et al., 2008).

Existing dates on hydrothermal alteration related to gold mineralization are spread over much of the Late Jurassic and

Early Cretaceous (Kistler et al., 1983; Böhlke and McKee, 1984; Böhlke and Kistler, 1986; Böhlke et al., 1989; Snow et al., 2008). Considering the complexity of the tectonic events in the Sierra Foothills during this time period, there are many questions concerning mode and duration of gold deposition.

GEOLOGY OF THE GOLD DISTRICTS

Most of the lode gold deposits of the Sierra foothills are hosted within metasedimentary and metavolcanic rocks of the Jura-Triassic arc belt and the overlying Upper Jurassic accretionary sequence (Snow and Scherer, 2006), and are located in second- and third-order faults adjacent to the regional Bear Mountain and Melones fault systems. Many of these local fault zones represent transpressional reactivation zones and dilational jogs that were developed within the regional first-order east-over-west thrust systems (Bierlein et al., 2008). The 165-km-long x 1- to 5-km-wide Mother Lode belt of deposits closely follows the trace of the Melones fault zone. Many of the Foothills gold deposits show a close spatial association with serpentinized ultramafic bodies exposed along the regional fault systems. In the Grass Valley district, the Empire deposit orebodies occur as conjugate vein sets within latest Jurassic or Early Cretaceous granodiorite and are about 25 km west of the main strand of the Melones fault zone. Samples for this study were collected from ores in the Downieville, Alleghany, Grass Valley, Confidence, Jamestown, Placerville, Hodgson, Coulterville, and Bagby districts. The Jamestown and Placerville districts make up a portion of the Mother Lode gold belt.

At the Sixteen-to-One deposit in the Alleghany district, auriferous ribbon-type quartz veins along a series of steep reverse faults contain pyrrhotite, pyrite, arsenopyrite, sphalerite, chalcopyrite, tetrahedrite, and galena, as well as ankerite, mariposite, and graphite, to depths of one km. Veins are hosted by highly-faulted Carboniferous metasedimentary rocks and mélangé of the Calaveras Formation that are intruded by serpentinite dikes (Bowen and Crippen, 1997), although elsewhere in the district (i.e., Oriental deposit)

high-grade veins cut granodiorite. The auriferous veins in the nearby Downieville district, such as those at the Oxford deposit, are also hosted by the same units of the Calaveras Formation. However, here pyrite-rich disseminated mineralization occurs in the wallrock and the veins, although containing abundant sulfides, contain less free gold than veins in Alleghany district (Carlson and Clark, 1956).

In Grass Valley, gold veins cut both granodiorite and Late Triassic-Middle Jurassic accreted metasedimentary rocks of the Slate Creek-Lake Combie and Fiddle Creek-Tuolumne River belt terranes (Johnston, 1940; Dickinson, 2008), which were accreted to the Calaveras mélangé belt along poorly understood structures such as the Gillis Hill and Dogwood faults (Day and Bickford, 2004). Böhlke and Kistler (1986) reported a hornblende K-Ar date for the granodiorite of 126.7 ± 3 Ma; more recently, Irwin and Wooden (2001) published a U/Pb age of 159 Ma. Relatively continuous (>1 km), high-grade veins within thrust faults occur in two generalized groups; steeply-dipping, northwest-trending, serpentinite- and amphibolite-hosted veins, such as the Idaho-Maryland deposit, and gently-dipping, granodiorite-hosted veins, such as the Empire deposit, which strike north and parallel to the length of the igneous body (Johnston, 1940). Veins in the Grass Valley district consist of quartz, calcite, and ankerite, with gold occurring as free grains and in pyrite, which is the most voluminous sulfide phase. The Grass Valley veins typically have a higher abundance of sulfide minerals relative to other gold districts in the Sierra foothills. Gold was historically mined to depths of more than 3 km, which is the deepest of any system within the Sierra foothills, with no obvious decrease in resource potential at the lowest mined depths.

Gold-rich quartz veins with minor pyrite in the Placerville district are hosted from east to west in rocks of the Calaveras Formation (Late Carboniferous and Triassic phyllite and chert), Mariposa Formation (Late Jurassic slate and greywacke), and a variety of mixed volcanic formations (greenstone and amphibolite; Clark, 2005). The main gold vein at Quartz Hill, just upstream from the Gold Bug mine, cuts the slate that is highly altered to a mariposite-ankerite-quartz assemblage. Much of the ankerite and pyrite has been oxidized by later supergene events.

Auriferous quartz-carbonate veins and stringers of the Mother Lode gold belt occur along both sides of the >350-km-long Melones fault zone, hosted by country rocks that include chert and argillite of the Calaveras complex; mélangé, ultramafic rocks, and volcanic and volcanoclastic rocks of the Jura-Triassic arc belt; and shale and fine-grained sandstones of the Upper Jurassic accretionary sequence of Ernst et al. (2008). The fault zone itself appears as a mylonitic tectonic mélangé with a diffuse series of faults along much of its length and was likely active during the same Early Cretaceous episode as the adjacent Bear Mountain fault system (see below). Flat extension veins that mutually cross-cut steep fault-veins indicate that the Melones zone behaved as a major reverse fault undergoing extreme fault-valve action (Sibson and Elliot, 1993).

Ribbon-type crack-seal quartz veins are common throughout the belt (Knopf, 1929). In the Jacksonville-Plymouth region of the Mother Lode, at Sutter Hill, gold-bearing quartz veins of the Comet-Lincoln vein system occur within slate or metavolcanic rocks that are commonly interbedded with greywacke of the Mariposa and Longtown Ridge Formations (Clark, 2005). The Carson Hill deposit is hosted by greenschist facies metavolcanic and clastic rocks directly within the Melones Fault Zone. Gold \pm telluride-rich quartz veins contain abundant pyrite and minor chalcopyrite, tetrahedrite, molybdenite, galena, and bornite. Associated alteration surrounding the mineralized veins is mainly sericite-ankerite-mariposite (Clark, 2005). The Jack Adit occurrence, near Tuttletown, and the Alameda deposit, north of Jamestown, like Carson Hill are hosted in highly-deformed phyllite, slate, schist, and serpentinite within the Melones fault zone. Ankerite-quartz-mariposite alteration is prevalent. Near Tuttletown, the ore veins contain pyrite, galena, and tellurides (Clark, 2005). The open pit of the Harvard deposit in Jamestown exposed a variety of ore-hosting units within the Melones fault zone: graphitic slate, phyllite, chlorite schist, greenstone, and serpentinite. Ankerite-, talc-, quartz-, and mariposite-bearing schist occur within alteration zones surrounding the fault zones (Neidig, 2001). Quartz Hill consists of a large quartz vein in a brittle fault that cuts the Melones fault zone, with serpentinite and metavolcanic rocks in the footwall and metasedimentary rocks in the hangingwall (Landefeld and Snow, 1990); it was mined to about 1.4 km depth.

The Royal Mountain King deposit is in the Hodson district and is the most significant gold deposit along the 300-km-long, 2- to 7-km-wide, east-dipping Bear Mountain fault system. Gold deposits along this fault system form the so-called "West Gold Belt", which parallels the Mother Lode belt that is located about 10 km to the east. The main period of deformation and metamorphism on both sides of the fault system has been well-constrained between 150 and 123 Ma (Tobisch et al., 1989; Miller and Paterson, 1991). The Royal Mountain King deposit occurs along the northwest-trending Hodson fault, a splay off the regional Bear Mountain fault (Landefeld and Snow, 1990). It is hosted in the Salt Springs slate and phyllite (Upper Jurassic accretionary sequence) and Copper Hill mafic volcanic rocks (Jura-Triassic arc belt), with some lenses of serpentinite within the fault structures. Most gold occurs in pyrite, which is disseminated in wallrocks, and some is also hosted in quartz veins and stockworks; sericite, ankerite, and mariposite are common alteration phases (Kuhl, 1989).

In the Coulterville district, at the McAlpine deposit, the footwall to the ore is sheared serpentinite with lenses of graphitic phyllite and the hangingwall is highly altered metaigneous rock. The gold mineralization is confined to quartz veins. Vein mineralogy includes quartz, ankerite, sericite, chlorite, and pyrite (Weir, 1986; Weir and Kerrick, 1987). The Pine Tree-Josephine deposit in the Bagby district is located directly within the highly deformed rocks of the Melones

fault zone and was the most southerly deposit sampled for this study. Much of the fault zone appears as a complex mélange of highly carbonate-altered greenstone, highly-sheared and serpentinized metagabbro, hornblende-rich metadiorite, and ankerite-quartz-mariposite-bearing schist, surrounded by argillites of the Mariposa Formation in the footwall to the west and the Bullion Mountain metavolcanic rocks to the east (McAllister, 1990). The auriferous veins, continuing for more than 350 m along strike, also contain pyrite and arsenopyrite with minor chalcopyrite, galena, millerite, sphalerite, and niccolite (Clark, 2005).

The Confidence mine is in the “East Gold Belt” and is hosted by Late Jurassic (ca. 162 Ma) granodiorite on the eastern edge of the Standard Pluton. Auriferous quartz veins strike north to northwest and contain gold and abundant sulfides including galena (Clark, 2005). This is the most easterly sampled gold occurrence in our study.

PREVIOUS GEOCHRONOLOGY

Published K-Ar ages of hydrothermal micas range from 143.7 ± 3 to 104 Ma and Rb-Sr ages on quartz and carbonate associated with auriferous quartz veins range from 140.9 ± 3 to 114.6 ± 3 Ma for deposits throughout the Sierra foothills (Table 1; Fig. 3). Those specifically from the Mother Lode

belt range between ca. 131 and 105 Ma (Kistler et al., 1983). However, the broad ranges may reflect relative imprecision with the dating methods. Using K-Ar, it is difficult to distinguish if samples analyzed contain excess argon, which likely would characterize some of the hydrothermal micas from this region due to the prolonged tectonic and metamorphic history. Similarly, it could be difficult to determine a homogenous initial Sr isotopic value in quartz and carbonate in a tectonically complex region.

Prior $^{40}\text{Ar}/^{39}\text{Ar}$ dating was done by Böhlke et al. (1989) using a laser microprobe of hydrothermal sericite in altered serpentinite adjacent to the ore veins at the Oriental deposit, Alleghany district. Three resulting dates were obtained of 118.0, 111.7, and 104.0 Ma, but it is not clear which of these dates represents the formation age of the deposit. The dates partially overlap the Rb-Sr and K-Ar dates from numerous deposits in the district of ca. 127-107 Ma, which had been previously measured by Böhlke and Kistler (1986).

In the Grass Valley district, Böhlke and Kistler (1986) reported anomalously old ages for mica and quartz from the Brunswick vein of 143.7 ± 3 and 140.9 ± 3 Ma. Although Böhlke (1999) pointed out the anomalous nature of these earliest Cretaceous dates for gold deposition in Grass Valley, Landefeld (1988) favored these older dates as the best approximation of gold formation throughout the Sierra foot-

Table 1. $^{40}\text{Ar}/^{39}\text{Ar}$ ages from previous studies.

District	Mine	Method	Mineral	Age (Ma)	Reference
Allegheny	Irelan	K-Ar	mariposite	112.9 ± 3	Böhlke and McKee (1984)
	Irelan	Rb-Sr	quartz	116.3 ± 3	Böhlke and Kistler (1986)
	Irelan	Rb-Sr	carbonate	115 ± 3	Böhlke and Kistler (1986)
	Rainbow Extension	K-Ar	mariposite	111.6 ± 3	Böhlke and McKee (1984)
	Plumbago	K-Ar	mica	112.5 ± 3	Böhlke and Kistler (1986)
	Gold Crown	Rb-Sr	carbonate	109.6 ± 3	Böhlke and Kistler (1986)
	Kate Hardy	Rb-Sr	carbonate	124.5 ± 3	Böhlke and Kistler (1986)
	Kate Hardy	Rb-Sr	quartz	124.2 ± 3	Böhlke and Kistler (1986)
	Oriental	Ar-Ar	mica	118	Böhlke et al (1989)
	Oriental	Ar-Ar	mica	104	Böhlke et al (1989)
	Oriental	Ar-Ar	mica	111.7	Böhlke et al (1989)
Sixteen to One	Ar-Ar	mariposite	127.5 ± 1.4	Snow et al (2008)	
Washington	Red Ledge	Rb-Sr	carbonate	119.4 ± 3	Böhlke and Kistler (1986)
	Red Ledge	K-Ar	mica	120.9 ± 4	Böhlke and Kistler (1986)
Grass Valley	Brunswick	Rb-Sr	quartz	140.9 ± 3	Böhlke and Kistler (1986)
	Brunswick	K-Ar	mica	143.7 ± 3	Böhlke and Kistler (1986)
	Idaho - Maryland	Ar-Ar	mariposite	152.2 ± 1.2	Snow et al (2008)
Mother Lode	Garibaldi	Rb-Sr	mariposite	114.6 ± 3	Kistler et al (1983)
	Garibaldi	K-Ar	mariposite	116.3 ± 3	Kistler et al (1983)
	Garibaldi	Ar-Ar	mariposite	121.2 ± 4.7	Snow et al (2008)
	Mary Harrison	K-Ar	mariposite	108 ± 3	Kistler et al (1983)
	Mary Harrison	K-Ar	mariposite	116 ± 3	Kistler et al (1983)
	Carson Hill	Ar-Ar	mariposite	134.8 ± 0.7	Snow et al (2008)
	Harvard	Ar-Ar	mariposite	130.9 ± 0.6	Snow et al (2008)
	Harvard/Jamestown	K-Ar	mariposite	127 ± 3	Kistler et al (1983)
	Coulterville road cut	Ar-Ar	mariposite	120.8 ± 1.5	Snow et al (2008)

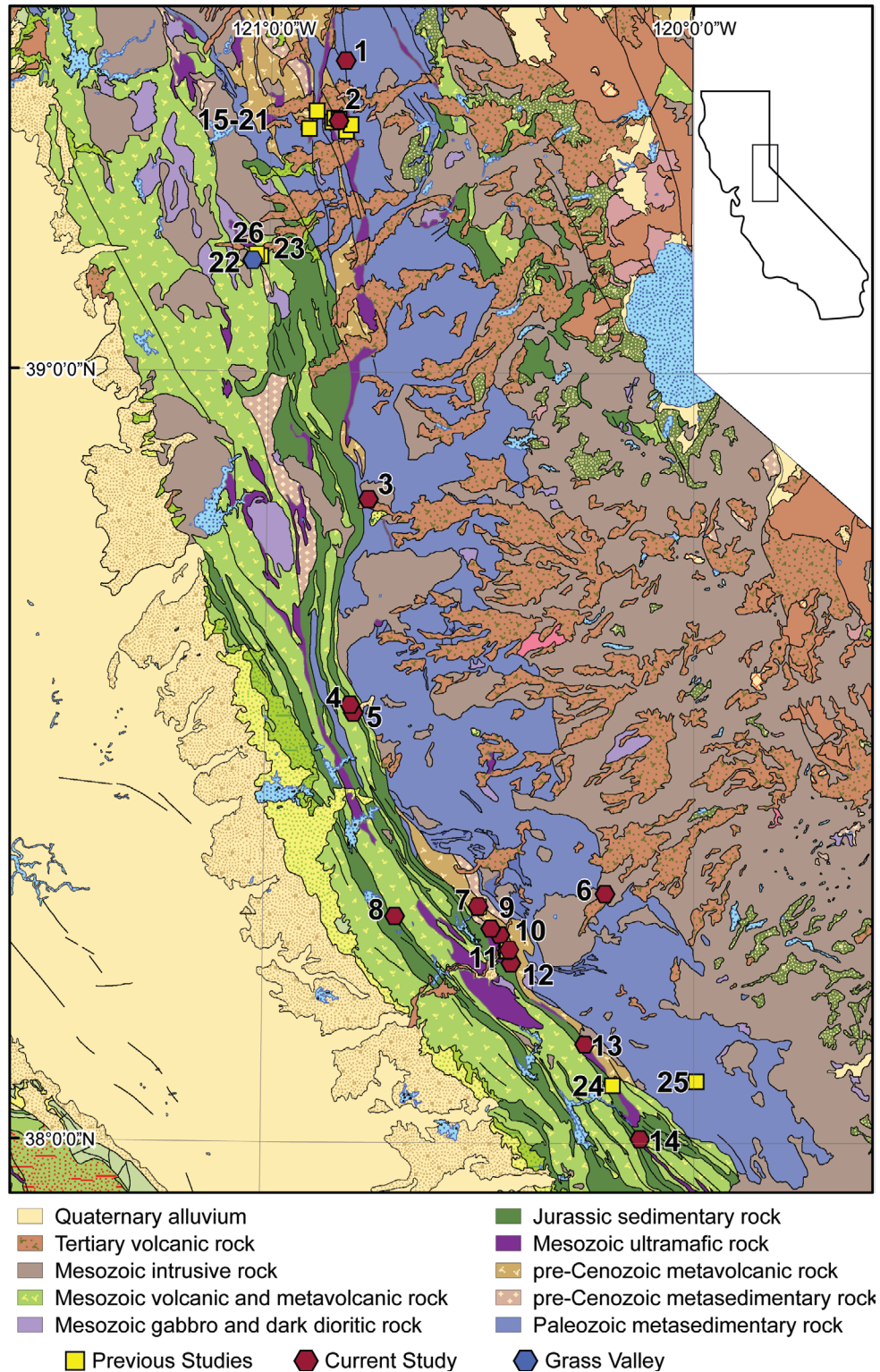


Figure 3. Sample locations: 1 – Oxford Mine; 2- Sixteen to One; 3 – Quartz Hill (Placerville district); 4 – Sutter Hill; 5 – Eureka; 6 – Confidence; 7 – Carson Hill; 8 – Royal Mountain King; 9 – Jack Adit; 10 – Alameda; 11 – Harvard; 12 – Quartz Hill; 13 – McAlpine; 14 – Pine Tree/Josephine; 15 – Kate Hardy; 16 – Red Ledge; 17 – Oriental; 18 – Plumbago; 19 – Irelan; 20 – Rainbow Extension; 21 – Gold Crown; 22 – Empire; 23 – New Brunswick; 24 – Mary Harrison; 25 – Garibaldi; 26 – Idaho-Maryland.

hills province. These dates on Grass Valley gold, in addition, are older than Böhlke and Kistler's (1986) date for the main granodiorite body in the district (126.7 ± 3 Ma), which significantly is the host unit to a number of auriferous veins that include those of the giant Empire deposit (Clark, 1984; Clark, 2005). This age discrepancy may be resolved by a recent U/Pb date of 159 Ma for the granodiorite of the Grass Valley pluton obtained by Irwin and Wooden (2001).

A more recent publication on the timing of gold deposition in the region by Snow et al. (2008) presents mariposite $^{40}\text{Ar}/^{39}\text{Ar}$ dates ranging from 134.8 ± 1.4 to 120.8 ± 1.5 Ma for deposits in the Mother Lode and Coulterville districts. In the Allegheny and Grass Valley districts, dates obtained from mariposite from the Sixteen to One and Idaho-Maryland deposits are 127 ± 1.4 and 152.2 ± 1.2 Ma, respectively.

CURRENT STUDY

Argon methods

Ten mariposite (a green chromium-rich variety of phengite) and one sericite sample were analyzed using the $^{40}\text{Ar}/^{39}\text{Ar}$ age-spectrum dating technique. Our samples are from the Sixteen to One and Oxford mines in the Allegheny district; the Harvard pit, Quartz Mountain, Jamestown, Carson Hill pit, Alameda, Quartz Hill, and Placerville mines in the Mother Lode district; the McAlpine deposit in the Coulterville district; Pine Tree/ Josephine mine in the Bagby district; and the Confidence mine in the Confidence district (Fig. 3). The analyses are of variable purity (95-99%) mineral separates. The primary impurity in all of the mariposite samples is intergrown and co-genetic sericite. The single sericite sample had a purity of >99%. The samples were crushed, ground, sieved, and concentrated using standard magnetic and density separation techniques. Final purity was accomplished using light duty ultrasonic abrading and cleaning, followed by additional magnetic and density separations and handpicking. All ages were determined at the U.S. Geological Survey argon-dating laboratories in Reston, Virginia. Analytical methods are discussed in detail by Haugerud and Kunk (1988) and Kunk and Burton (1999).

Prior to analysis, the samples were irradiated at the U.S. Geological Survey TRIGA reactor (Dalrymple et al., 1981). The standard MMhb-1, with an age of 519.4 Ma (Alexander et al., 1978; Dalrymple et al., 1981), was used as the fluence monitor. The samples were incrementally heated in a low-blank furnace, similar to that described by Staudacher et al. (1978), for ten minutes per step. After removing reactive gases, each heating step was analyzed in a VG MM 1200b mass spectrometer, operated in the static mode. Data reduction was accomplished using an updated version of the program ArAr* (Haugerud and Kunk, 1988) and the decay constants recommended by Steiger and Jäger (1977). Plateau ages, when they occur, are defined using the criteria of Fleck et al. (1977) as modified by Haugerud and Kunk (1988). They include 50%

or more of the ^{39}Ar released from the age spectrum in two or more contiguous steps that agree in age with one another within the limits of analytical precision. Inverse isochrons were calculated for samples using the method of York (1969). For an inverse isochron age to be considered meaningful, it was required to contain >50 percent of the ^{39}Ar released from the sample, and have a MSWD (Mean Square Weighted Deviate) of <2.5 and a calculated initial $^{40}\text{Ar}/^{36}\text{Ar}$ ratio of >295.5. If these criteria were not met, individual points were deleted from the low and(or) high temperature part of the analysis to improve the fit. Several of the inverse isochrons did not give meaningful results (as noted in Fig. 4) and are not presented.

Argon results

Analytical results for these samples are listed in Table 2 and the Appendix. All uncertainties in these tables are at 1 sigma. A graphical representation of these results is shown in Figure 4; there are three graphs for each sample. On the left is the age spectrum diagram, which presents the percent of $^{39}\text{Ar}_K$ released against apparent age in millions of years. The height of the boxes in this diagram represents the 2σ uncertainty of the analysis. The box width represents the percent $^{39}\text{Ar}_K$ released for each step. Above this, the apparent K/Ca ratio of each step is plotted against percent $^{39}\text{Ar}_K$ released. On the right is the inverse isotope correlation diagram that displays $^{39}\text{Ar}/^{40}\text{Ar}$ against $^{36}\text{Ar}/^{40}\text{Ar}$. Included in this figure is the apparent age of the sample (calculated from the inverse of the X-axis intercept), if the above criteria were met, the initial $^{40}\text{Ar}/^{36}\text{Ar}$ ratio (the inverse of the Y-axis intercept), the MSWD, and the points that were excluded from the above mentioned calculations. For additional information on the sample data sets, see Haugerud and Kunk (1988).

Table 2. $^{40}\text{Ar}/^{39}\text{Ar}$ ages reported in this study.

District	Mine	Mineral	Age (Ma)
Allegheny	Sixteen to One	mariposite	114.7 ± 1.4
	Oxford	mariposite	117.3 ± 0.8
Mother Lode	Royal Mountain King	mariposite	125.4 ± 0.2
	Sutter Hill	muscovite	129.8 ± 2.3
	Harvard pit	mariposite	129.9 ± 0.7 129.8 ± 0.8
	Quartz Mountain, Jamestown	mariposite	129.7 ± 0.7 128.5 ± 1.3
	Carson Hill Pit	mariposite	134.3 ± 1
	Alameda	mariposite	130.4 ± 1.5
	Quartz Hill, Placerville	mariposite	123.5 ± 1.1
	Jack Adit	mariposite	124.3 ± 0.7
Coulterville	McAlpine	mariposite	~ 123
Bagby	Pine Tree/Josephine	mariposite	115.6 ± 1.3
Confidence	Confidence	muscovite	128.2 ± 0.7

The age spectrum of the mariposite sample from Sixteen-to-One deposit is slightly U-shaped (Fig. 4A), suggesting the presence of excess argon in the sample. The minimum age in the "U" is 114.7 Ma and represents a maximum age for the sample. Inverse isotope correlation of these data, deleting points A, B, and P (which have noticeably lower K/Ca ratios than the rest of the steps in the age spectrum) and subsequently containing 98 percent of the $^{39}\text{Ar}_K$ released, results in an age of 114.7 ± 1.4 Ma, with an MSWD of 0.143 and an initial $^{40}\text{Ar}/^{36}\text{Ar}$ of 655 ± 370 . Although the uncertainty on the initial $^{40}\text{Ar}/^{36}\text{Ar}$ is quite large, the radiogenic yields of the other steps fairly tightly constrain the uncertainty of the apparent age. We interpret this 114.7 ± 1.4 Ma date, which is in agreement with the 114.7 Ma minimum age step, to represent the age of this sample.

Except for the first temperature step, the age spectrum of mariposite from the Oxford deposit is also U-shaped with a minimum age of 117.2 Ma (Fig. 4B). Inverse isotope correlation analysis of these data, excluding points A and B and containing 97.2 percent of the $^{39}\text{Ar}_K$ released, results in an age of 117.3 ± 0.8 Ma, with an MSWD of 0.356 and an initial $^{40}\text{Ar}/^{36}\text{Ar}$ of 373 ± 51 . The inverse isochron age of 117.3 ± 0.8 Ma is interpreted as the age of the sample.

The age spectrum of mariposite from the Harvard pit climbs in age in its first four heating steps and decreases in age in the following two steps before developing an age plateau of 129.9 ± 0.7 Ma in the 875-1100°C steps that contain 80.8 percent of the $^{39}\text{Ar}_K$ released (Fig. 4C). Inverse isotope correlation analysis of this data, excluding points A and B and containing 94.6 percent of the $^{39}\text{Ar}_K$ released, results in an age of 129.8 ± 0.8 Ma with an MSWD of 0.275 and an initial $^{40}\text{Ar}/^{36}\text{Ar}$ of 506 ± 166 . The plateau age, 129.9 ± 0.7 Ma, is interpreted to be the age of this sample.

The age spectrum of mariposite from Quartz Mountain, Jamestown district climbs in age from 42 Ma to 129 Ma and then develops an age plateau of 129.7 ± 0.7 Ma in the 700 - 825°C steps that includes 63 percent of the $^{39}\text{Ar}_K$ released (Fig. 4D). Inverse isotope correlation analysis of these data, excluding points A, B, O and P and containing 96.6 percent of the $^{39}\text{Ar}_K$ released, results in an age of 128.5 ± 1.3 Ma, with an MSWD of 0.260 and an initial $^{40}\text{Ar}/^{36}\text{Ar}$ of 408 ± 178 . The plateau age, 129.7 ± 0.7 Ma, is interpreted to be the age of this sample.

The age spectrum of mariposite from the Carson Hill pit climbs in age from 103 Ma in the 500°C step to 136 Ma in the 825°C, and then bounces in age between 134 Ma and 137 Ma in the remainder of the spectrum (Fig. 4E). Inverse isochron correlation analysis of these data, excluding points A, B, and C and including 92.8 percent of the $^{39}\text{Ar}_K$ released, results in an age of 134.3 ± 1.0 Ma, with an MSWD of 0.707 and an initial $^{40}\text{Ar}/^{36}\text{Ar}$ of 588 ± 166 . The inverse isochron age is interpreted as the age of this sample.

The age spectrum of mariposite from the Alameda deposit climbs in age from 39 Ma in the 500°C step to 133 Ma in the 750°C step then decreases in age to 130 Ma in the 925°C step and finally climbs to 163 Ma in the last step (Fig.

4F). Inverse isotope correlation analysis of these data, excluding points A and B and including 98.0 percent of the $^{39}\text{Ar}_K$ released, results in an age of 130.4 ± 1.5 Ma, with an MSWD of 0.137 and an initial $^{40}\text{Ar}/^{36}\text{Ar}$ of 643 ± 239 . The inverse isochron age is interpreted as the age of this sample.

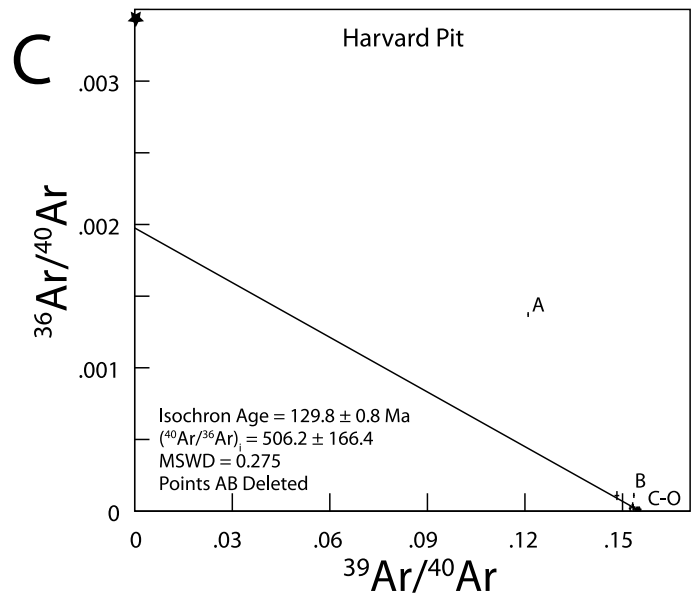
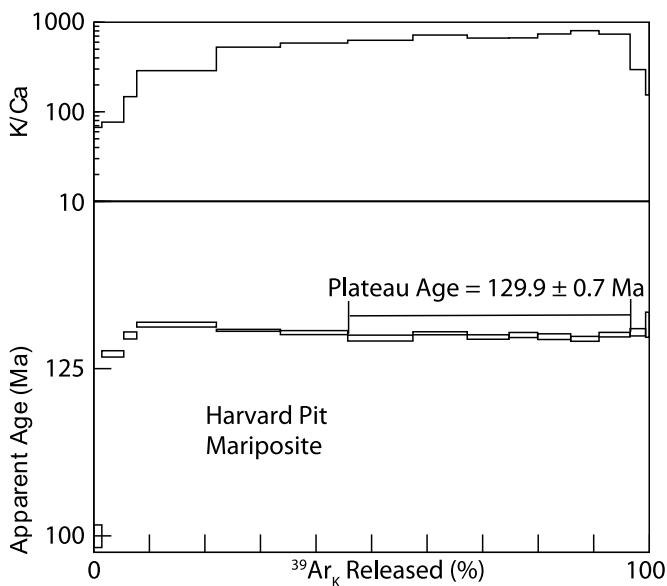
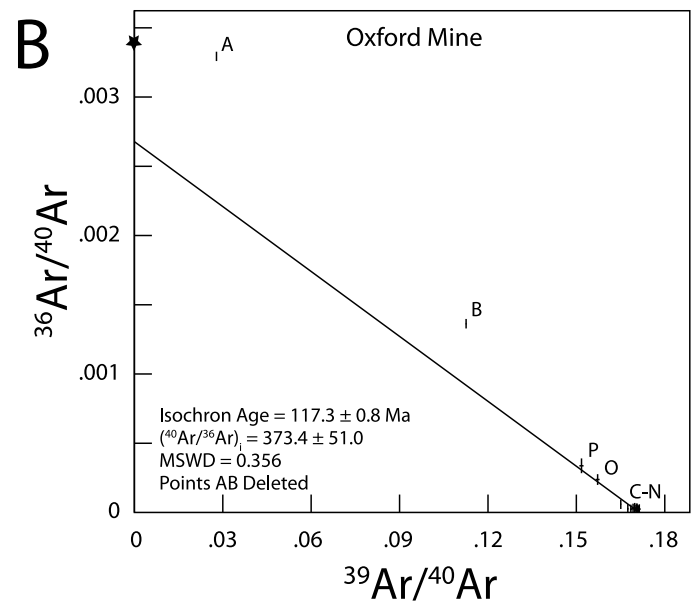
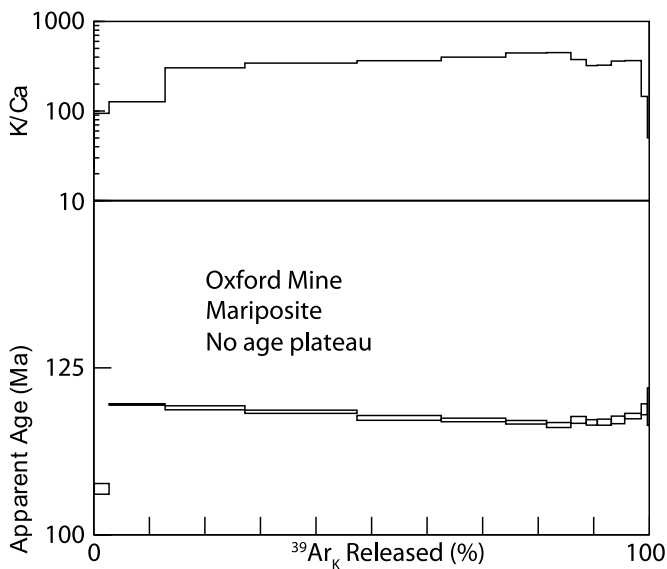
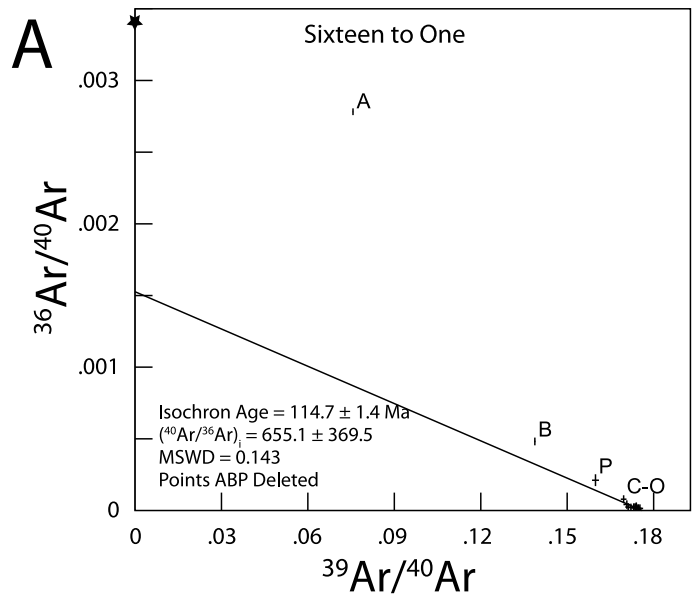
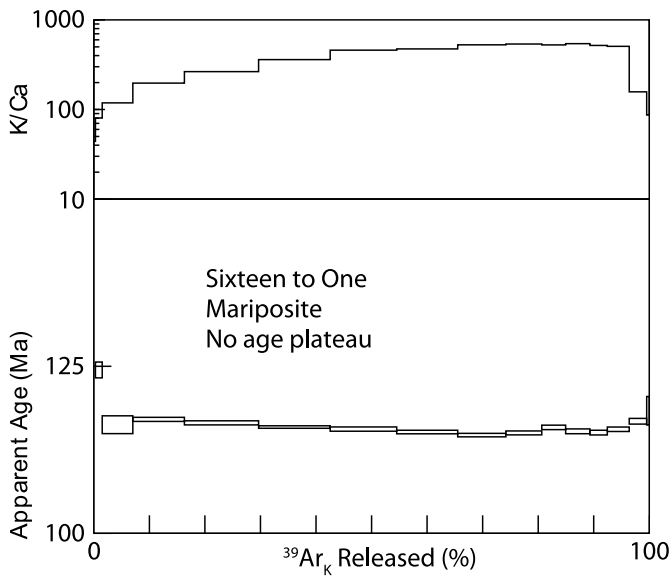
The age spectrum of mariposite from Quartz Hill in the Placerville district climbs from 49 Ma in the 500°C step to 127 Ma in the 700°C step (Fig. 4G). With the exception of the last step, ages range between 123 and 125 Ma, but no age plateau is developed. The last step has an apparent age of 145 Ma. The K/Ca ratios of this sample are much lower than those for the other samples in this study and call into question the validity of these data. Nonetheless, inverse isotope correlation analysis of these data, excluding points A, B, and P and including 98.0 percent of the $^{39}\text{Ar}_K$ released, results in an age of 123.5 ± 1.5 Ma, with an MSWD of 0.110 and an initial $^{40}\text{Ar}/^{36}\text{Ar}$ of 713 ± 318 . The inverse isochron age is interpreted as the age of this sample.

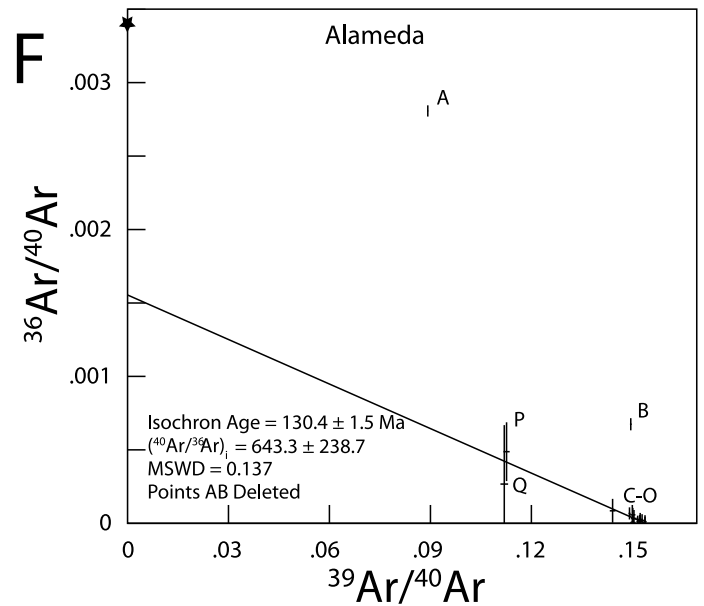
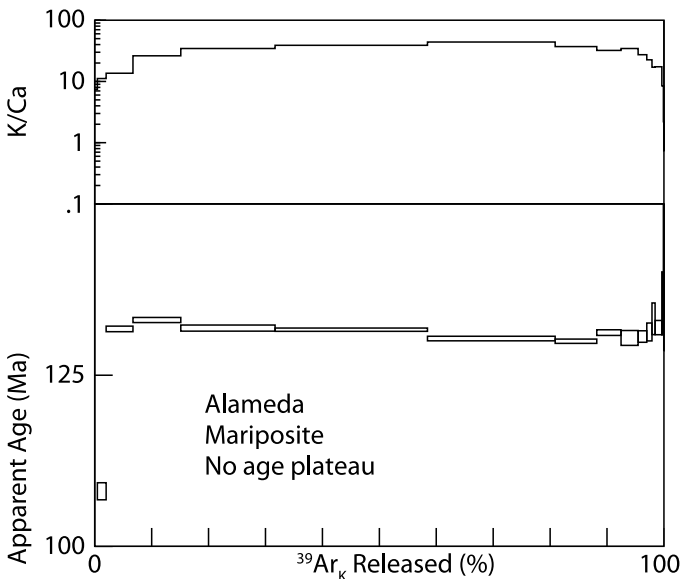
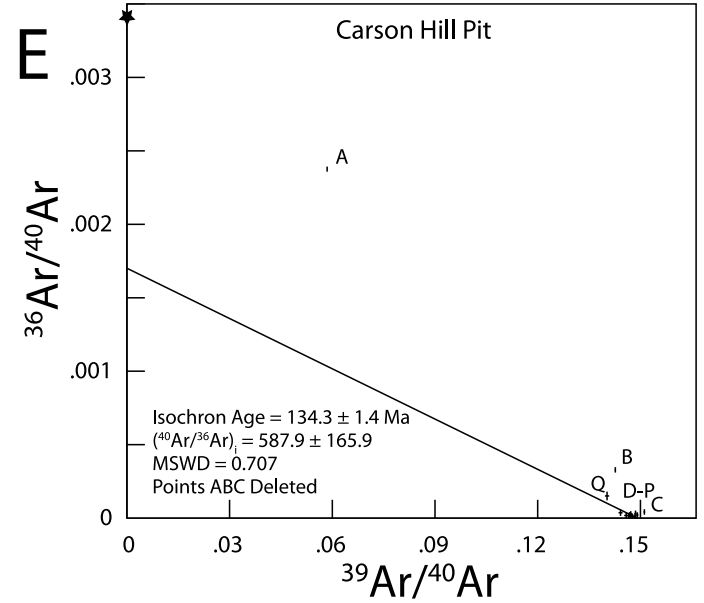
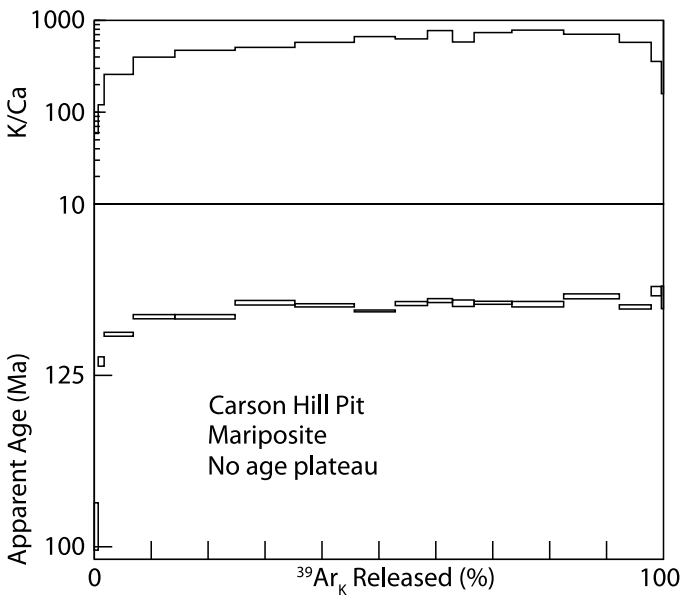
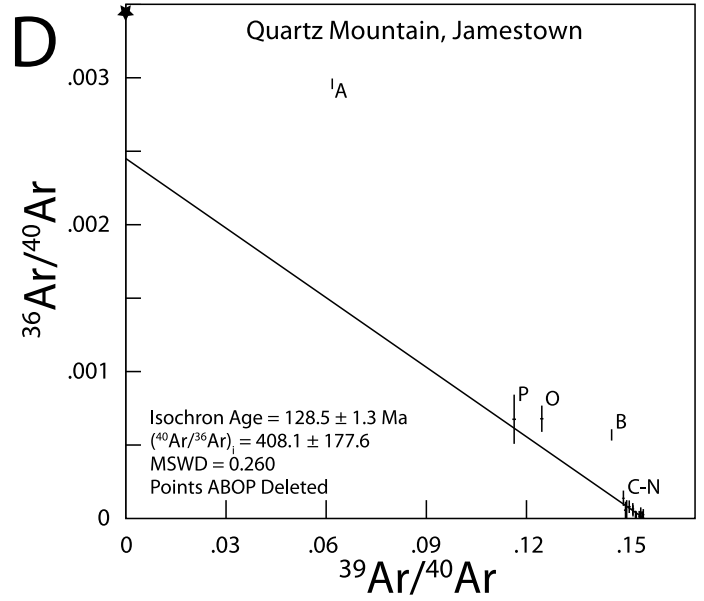
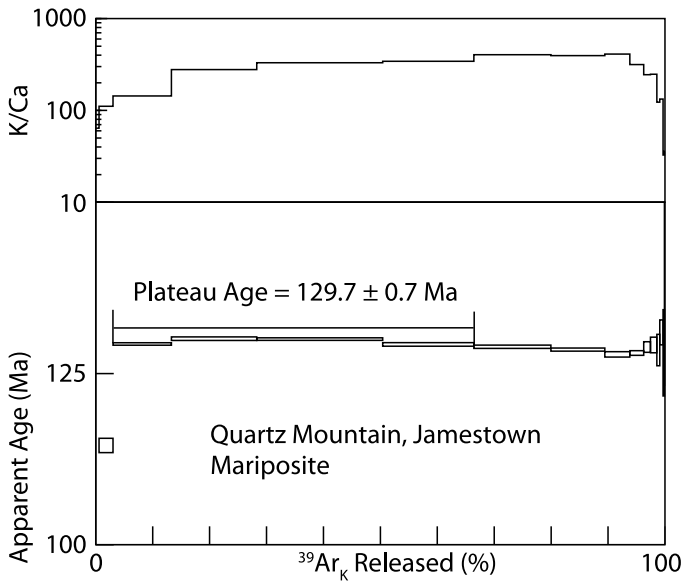
The mariposite from the McAlpine deposit yielded a disturbed age spectrum with ages ranging between 110 Ma and 136 Ma (Fig. 4H). Inverse isochron analysis of these data did not yield any useful results. The total gas age of ~123 Ma is interpreted to be the best estimate of the age of this sample.

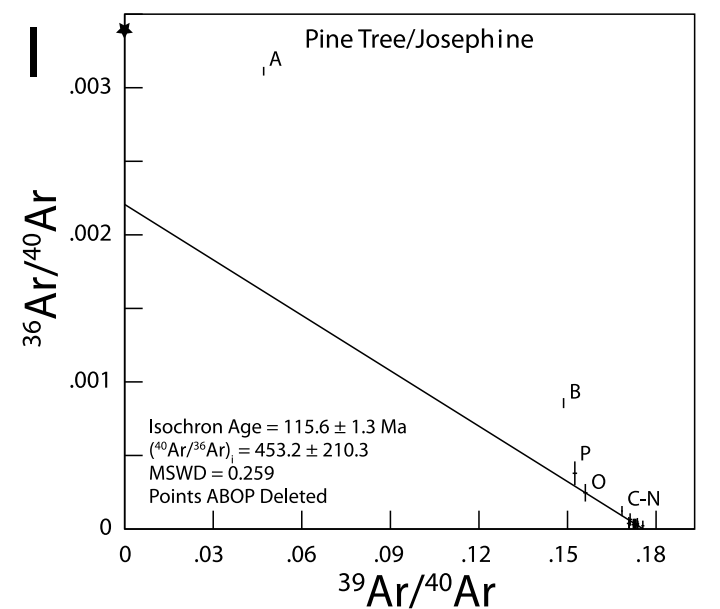
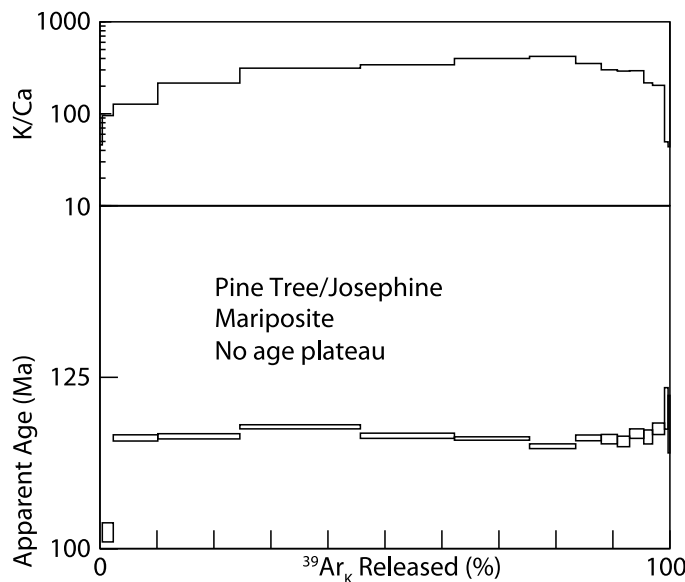
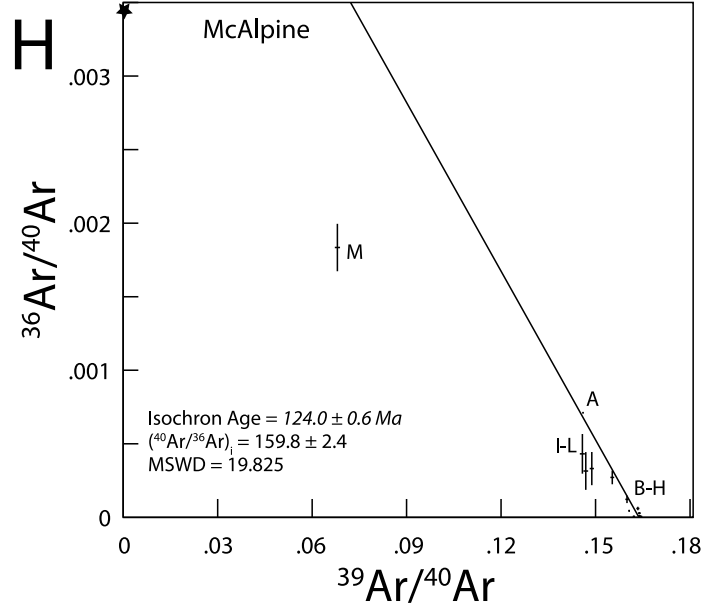
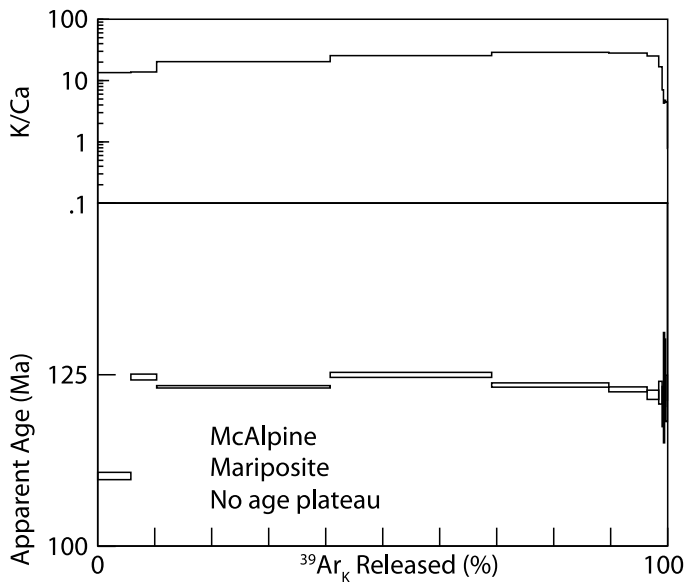
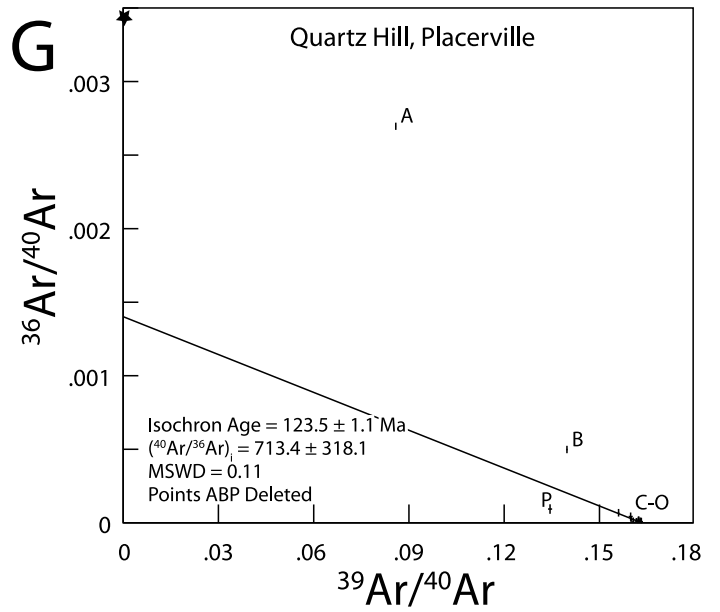
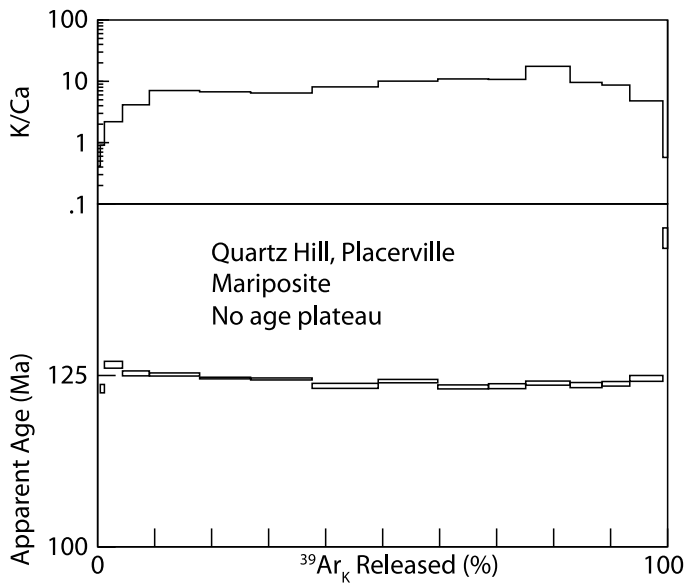
The age spectrum of mariposite from the Pine Tree/Josephine deposit climbs from 35 Ma in the 500°C step to 118 Ma in the 800°C step, then decreases to 115 Ma in the 875°C and finally climbs to 120 Ma in the 1250°C step without developing an age plateau (Fig. 4I). Inverse isotope correlation analysis of these data, excluding points A, B, O, and P and including 96.7% of the $^{39}\text{Ar}_K$ released, results in an age of 115.6 ± 1.3 Ma, with an MSWD of 0.259 and an initial $^{40}\text{Ar}/^{36}\text{Ar}$ of 453 ± 210 . The inverse isochron age is interpreted as the age of this sample.

The age spectrum of sericite from Confidence deposit climbs from 30 Ma in the 500°C step to 133 Ma in the 800°C step, then decreases to a plateau age of 128.2 ± 0.7 Ma that contains 61.2 percent of the $^{39}\text{Ar}_K$ released (Fig. 4J). Inverse isochron analysis of these data did not yield any useful results. The plateau age of 128.2 ± 0.7 Ma is interpreted as the age of this sample.

Mariposite occurs within the quartz-mica-ankerite alteration assemblage associated with the auriferous veins in the Sierra foothills. This alteration assemblage forms in serpentinite country rocks. The reported temperature of hydrothermal activity and gold deposition ranges from 250° to 380°C, but has a distinct mode near 300°C (Weir and Kerrick, 1987; Marshall and Taylor, 1980; Kistler et al., 1983; Böhlke, 1999). Because this temperature is below the closure temperature of muscovite-phengite of 350° - 400°C (McDougall and Harrison, 1999; Montigny, 1989), it is reasonable to assume that $^{40}\text{Ar}/^{39}\text{Ar}$ values reported here are crystallization ages of the micas and are not any type of cooling ages.







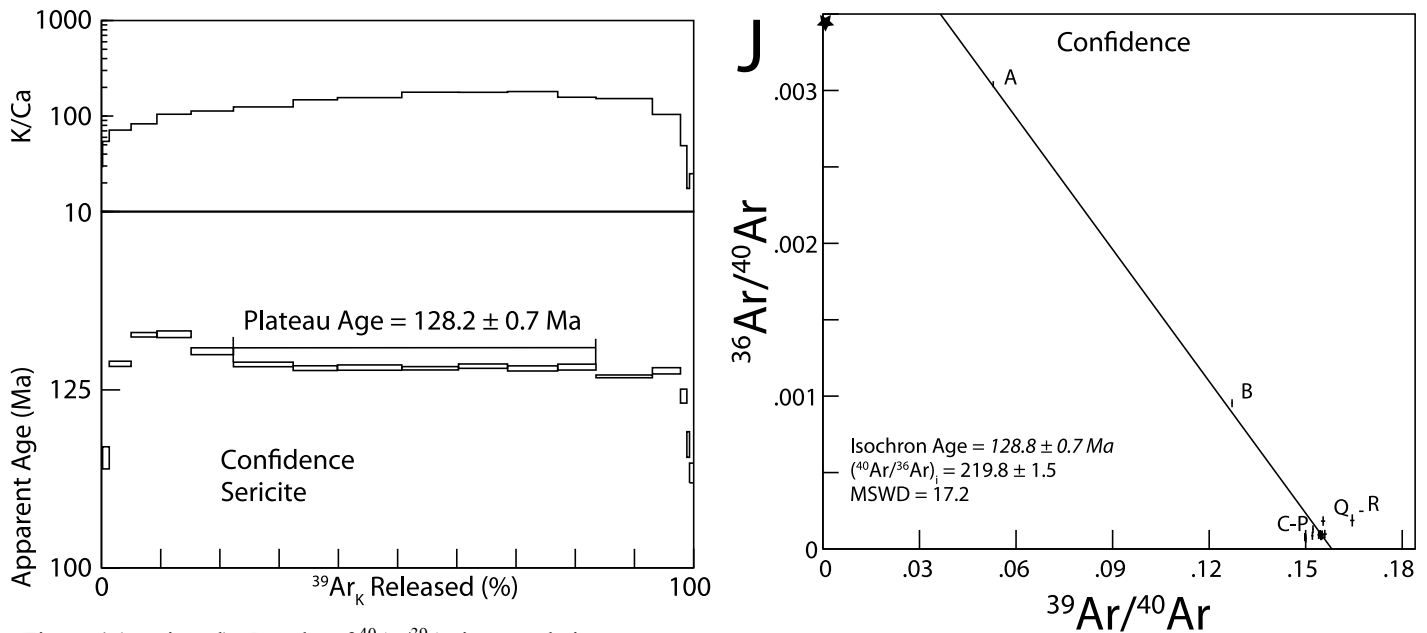


Figure 4 (continued). Results of $^{40}\text{Ar}/^{39}\text{Ar}$ isotope dating.

In addition, two remaining samples, from the Royal Mountain King and Sutter Hill orebodies, were collected and analyzed previously by Larry Snee (U.S. Geological Survey) and Jingwen Mao (Chinese Academy of Geological Sciences), respectively. Their unpublished argon plateau ages are both reported here with the other new argon data.

Dates for five deposits of the main Mother Lode gold belt, including the previous Sutter Hill date, cluster remarkably tightly between 134.3 ± 1.0 and 128.5 ± 1.3 Ma. There is no evidence for younger Aptian-Albian (119–97 Ma) gold events, as had been suggested by past K–Ar and Rb–Sr work (Böhlke and Kistler, 1986). Farther north along the Melones fault system, gold deposition in the Placerville district is estimated at 123.5 ± 1.1 Ma and, to the south, younger dates along the fault zone were also measured at McAlpine (ca. 123 Ma) and Pine Tree/Josephine (115.6 ± 1.3 Ma) deposits. Along the Bear Mountain fault system to the west, a date of 125.4 ± 0.2 Ma for the Royal Mountain King deposit is slightly younger than all those of the main Mother Lode belt. Gold ores of the East gold belt are similar in age to the Mother Lode ores of the “West gold belt”, as a 128.2 ± 0.7 Ma date characterizes the Confidence deposit within the margin of the Sierra batholith. Younger dates of 117.3 ± 0.8 and 114.7 ± 1.4 Ma characterize deposits of the Downieville and Alleghany districts at the northern end of the Sierra goldfields. These dates are consistent with those of Böhlke and Kistler (1986) for systems at the northern end of the gold province.

Rhenium-osmium

Much of the mineralization in the Sierra Foothills province is associated with pyrite and arsenopyrite. Rhenium-

osmium (Re–Os) analysis of sulfides has become a robust, direct method for dating gold mineralization that is interpreted to be coeval with sulfide deposition (Arne et al., 2001; Kirk et al., 2002; Selby et al., 2002; Morelli et al., 2005). To supplement our argon measurements of the timing of gold deposition in the Sierra foothills, arsenopyrite and pyrite separates from seven deposits were also examined by Re–Os analysis. This was particularly important given the uncertainties, described above, for the economically significant Grass Valley district, and the fact that suitable mica for argon dating could not be obtained from either the Idaho–Maryland or Empire orebodies in the district.

To determine if full Re–Os analysis was possible, a small amount of each of the sulfide samples was initially analyzed for Re abundance by isotope-dilution mass spectrometry (Table 3). Unfortunately, the sample submitted from the Empire orebody in the Grass Valley district did not have enough Re to allow for a full Re–Os analysis, nor did five other sulfide samples from the gold province. Only pyrite from Jack Adit occurrence, in the center of the Mother Lode belt, yielded enough radiogenic ^{187}Os to determine a Re–Os age. The Jack Adit sample was processed and isotopic composition was determined as described in Morelli et al. (2005, and references therein).

The age of pyrite formation at the Jack Adit occurrence, based upon the Re–Os dating, was measured to be 149.3 ± 1.5 Ma (Fig. 5). This date is significantly older than the $^{40}\text{Ar}/^{39}\text{Ar}$ age of fuchsite from the same sample, which was 124.3 ± 0.7 Ma. It is difficult to discern the reason for a 25 m.y. discrepancy between the two methods. The argon data yielded an overall range between 130.4 ± 1.5 and 114.7 ± 1.4 Ma, without any hint of a Late Jurassic event. They are not

Table 3. Rhenium content of pyrite from Sierra Foothills

Mine	Re ppb
Eureka	0.0
Empire	1.07
Carson Hill	0.32
Harvard Pit	1.2
Pine Tree/Josephine	0.27
Sixteen to One	2.4
Sixteen to One	0.6
Jack Adit	175
Jack Adit duplicate	362

cooling profiles, nor is it realistic to interpret their narrow age range as the age of uplift. The ca. 125 Ma period corresponds well with regional fault kinematics, certainly more so than the 149.3 ± 1.5 Ma age. Our preferred interpretation is that the pyrite is a pre-gold, country rock pyrite that was incorporated with other wallrock fragments into the vein during periods of hydrofracturing and vein formation. This is supported by the fact that the country rock at the Jack Adit occurrence is characterized by significant amounts of coarse-grained diagenetic pyrite and the fact that the high Re concentrations of this pyrite differ from that of all other pyrite and arsenopyrite grains studied from the goldfields. Weir and Kerrick (1987) discuss the timing and generations of pyrite at the McAlpine and Oro Rico deposits. They observed reduced Ni values in vein pyrite compared with pyrite in the alteration zone.

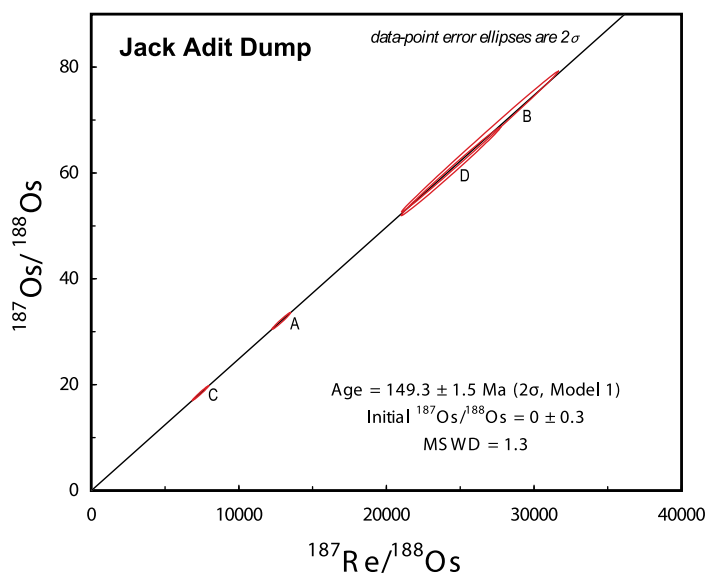


Figure 5. Re-Os isotope profile of sample from Jack Adit occurrence.

DISCUSSION AND CONCLUSIONS

Early Cretaceous gold of the Melones and related fault systems

Along with the new data from Snow et al. (2008), our ages show clearly that the bulk of the gold resource within the Mother Lode belt, centered along the Melones fault system, was deposited ca. 130 Ma. This overlaps with the final 10 m.y. of ductile deformation and regional metamorphism in the Sierra foothills, post-dates the final major pulse of Late Jurassic foothills magmatism by about 10 m.y., and pre-dates the onset of massive batholith emplacement by about 10 m.y. (e.g., Tobisch et al., 1989; Glazner, 1991). Faults to the east and west of the Melones also were sites of hydrothermal activity at about 130-125 Ma, as the regional stress fields shifted, dextral strike-slip was initiated, and important dilational zones were developed along the foothills fault systems (e.g., Bierlein et al., 2008). Gold deposition continued for 10 m.y. subsequent to the onset of dextral slip, as recorded by the ca. 115 Ma dates to the south along the Melones fault system and to the north in the Alleghany and Downieville districts along the northern parts of the fault system.

Previous data hinted at a younging of gold ages landward, with ages of gold mineralization to the west in Grass Valley perhaps being older than those of the Mother Lode belt along the Melones fault zone, and those furthest east, such as in the Alleghany district, being youngest. This would correlate with the long recognized observation that deformation along the fault zones becomes younger to the east, with those in the western foothills being active at the end of the Jurassic to those along the Sierra crest being the focus of deformation in mid-Cretaceous. However, some of our new argon data show that, at least to the south, gold ages essentially overlap between deposits along the Bear Mountain fault system to the west, along the Melones fault system in the center, and within the East Gold belt to the east. Thus Grass Valley seems to be the only important temporally distinct district within the Sierra foothills province.

As discussed by Goldfarb et al. (2007), a major shift in plate motion in the Pacific basin may have been the driving force for much of the gold mineralization along the Melones, Bear Mountain, and related fault systems between the accreted terranes. The time at ca. 125 ± 10 Ma corresponds to a period of major change in far-field stresses, which caused significant changes in both convergence direction and convergence rates of the Farallon and North American plates. Resulting seismic activity focused fluid flow, and thus gold vein formation, into areas of transpressional reactivation and dilational jogs along the major fault systems. This activity was coeval with the immense Ontong-Java plume head reaching the underside of the Pacific Plate in the southern Pacific region, which caused reorganization of the Pacific basin plates, likely affecting the Farallon-North American plate boundary and being the ultimate cause of the above mentioned tectonism (Goldfarb et al.,

2007, 2008). Coeval uplift of the gold province, as supported by ages of much of the sediment of the Great Valley Group to the west of the foothills, may have facilitated fluid flow and vein formation events.

Late Jurassic gold of the Grass Valley district

The tectonomagmatic setting of the Late Jurassic Grass Valley orebodies appears unique relative to the other gold-rich parts of the Sierra foothills province. The district is located within the same western belt of metamorphic rocks as are the deposits of the Mother Lode belt to the south, but is a few tens of kilometers west of the Melones fault system that controls much of the Mother Lode resource. Grass Valley is also localized within an area of the belt characterized by widespread Late Jurassic plutonism, an event that was much less common in areas of Early Cretaceous goldfields to the south and in the vicinity of the Alleghany district to the northwest. Noteworthy, however, is the fact that these Middle to Late Jurassic plutons are also widespread in the auriferous parts of the Klamath Mountains, a few hundred kilometers to the northwest.

The anomalously old gold mineralization in the world-class Grass Valley district formed sometime between ca. 152 and 143 Ma (Böhlke and Kistler, 1986; Snow et al., 2008). This time range also overlaps with the date of ca. 147 Ma for the Quartz Hill deposit in the Klamath Mountains gold province of northern California, as first pointed out by Elder and Cashman (1992). Numerous correlations have been made between the geology, age, and structures of the northern Sierra Nevada and Klamath Mountains (e.g., Saleeby, 1990; Fagan et al., 2001; Irwin, 2003; Snow and Scherer, 2006, Ernst et al., 2008). The auriferous veins of the Quartz Hill and other deposits in the Klamath Mountains, responsible for about 7 million ounces of past gold production (Elder and Cashman, 1992), are hosted by the mafic volcanic and sedimentary rocks of the North Fork terrane, which correlates with those of the Slate Creek arc terrane in the Grass Valley district (Snow and Scherer, 2006; Ernst et al., 2008).

The complex Jurassic evolution of the northernmost Sierra foothills remains poorly understood, mainly because of Cretaceous and younger cover. At the end of the Jurassic, correlative with the gold event, the Sierra foothills and Klamath Mountains were offset 200 km by sinistral shear (Ernst et al., 2008) or by some complex type of forearc normal faulting (Dickinson, 2008). This dramatic offset of the pre-Cretaceous terranes was synchronous with ore formation in Grass Valley and the Klamath Mountains, most likely in favorable dilational zones often near the margins of slightly older plutons.

ACKNOWLEDGMENTS

We greatly appreciate the following individuals for kindly allowing access to properties and information; Robert Pease, Keith Testerman, Ross Grunwald, Jerry Pressler, Brad

Mark, Mark Payne, Ray Wittkopp, Rae Bell, David Arbogast, and Huw Northover. Jingwen Mao is thanked for dating of the Sutter Creek deposit. Mike Cosca provided a notably thorough review of this manuscript.

REFERENCES CITED

- Alexander, E.C., Jr., Mickelson, G.M., and Lanphere, M.A., 1978, MMhb-1: A new $^{40}\text{Ar}/^{39}\text{Ar}$ dating standard: U.S. Geological Survey Open-File Report 78-0701, p. 6-8.
- Arne, D.C., Bierlein, F.P., Morgan, J.W., and Stein H.J., 2001, Re-Os dating of sulfides associated with gold mineralization in central Victoria, Australia: *Economic Geology*, v. 96, p. 1455-1459.
- Bierlein, F.P., Northover, H.J., Groves, D.I., Goldfarb, R.J., and Marsh, E.E., 2008, Controls on mineralisation in the Sierra Foothills gold province, central California, USA – a prospectivity analysis: *Australian Journal of Earth Sciences*, p. 61-78.
- Böhlke, J.K., 1999, Mother Lode gold, *in* Moore, E.M., Sloan, D., and Stout, D.L., eds., *Classic Cordilleran Concepts – A View from California*: Geological Society of America Special Paper 338, p. 55-67.
- Böhlke, J.K., and Kistler, R.W., 1986, Rb-Sr, K-Ar, and stable isotope evidence for the ages and sources of fluid components of gold-bearing quartz veins in the northern Sierra Nevada Foothills Metamorphic Belt, California: *Economic Geology*, v. 81, p. 296-322.
- Böhlke, J.K., and McKee, E.H., 1984, K-Ar ages relating to metamorphism, plutonism, and gold-quartz vein mineralization near Alleghany, Sierra County, California: *Isochron-West*, n. 39, p. 3-7.
- Böhlke, J.K., Kirshbaum, C., and Irwin, J.J., 1989, Simultaneous analyses of noble gas isotopes and halogens in fluid inclusions in neutron-irradiated quartz veins using a laser microprobe noble gas mass spectrometer: U.S. Geological Survey Bulletin 1890, p. 61-80.
- Bowen, O.E., Jr., and Crippen, R.A., Jr., 1997, California's Mother Lode, north San Juan to Sattley, El Dorado, Placer, and Nevada Counties: *California Geology*, v. 6, p. 178-186.
- Carlson, D.W., and Clark, W.B., 1956, Lode gold mines of the Alleghany-Downieville area, Sierra County, California: *California Journal of Mines and Geology*, v. 52, p. 237-272.
- Clark, W.B., 1984, Gold mines of Grass Valley, Nevada County, California: *California Geology*, v. 4, p. 43-53.
- Clark, W.B., 2005, Gold districts of California: *Geological Survey of California Bulletin* 193, 199 p.
- Dalrymple, G.B., Alexander, C., Jr., Lanphere, M.A., and Kraker, G.P., 1981, Irradiation of samples for $^{40}\text{Ar}/^{39}\text{Ar}$ dating using the Geological Survey TRIGA reactor: U.S. Geological Survey Professional Paper 1176, 55 p.
- Day, H.W., and Bickford, M.E., 2004, Tectonic setting of the Jurassic Smartville and Slate Creek complexes, northern Sierra Nevada, California: *Geological Society of America Bulletin*, v. 116, p. 1515-1528.
- Dickinson, W.R., 2004, Evolution of the North American Cordillera: *Annual Review of Earth and Planetary Sciences*, v. 32, p. 13-45.
- Dickinson, W.R., 2008, Accretionary Mesozoic-Cenozoic expansion of the Cordilleran continental margin in California and adjacent Oregon: *Geosphere*, v. 4, n. 2, p. 329-353.
- Elder, D., and Cashman, S.M., 1992, Tectonic controls and fluid evolution in the Quartz Hill, California, lode gold deposits: *Economic Geology*, v. 87, p. 1795-1812.
- Ernst, W.G., Snow, C.A., Scherer, H.H., 2008, Contrasting early and late Mesozoic petro-tectonic evolution of northern California: *Geological Society of America Bulletin*, v. 120, p. 179-194.

- Fagan, T.J., Day, H.W., and Hacker, B.R., 2001, Timing of arc construction and metamorphism in the Slate Creek Complex, northern Sierra Nevada, California: *Geological Society of America Bulletin*, v. 113, p. 1105-1118.
- Fleck, R.J., Sutter, J.F., and Elliot, D.H., 1977, Interpretation of discordant $^{40}\text{Ar}/^{39}\text{Ar}$ age-spectra of Mesozoic tholeiites from Antarctica: *Geochimica et Cosmochimica Acta*, v. 41, p. 15-32.
- Glazner, A.F., 1991, Plutonism, oblique subduction, and continental growth: An example from the Mesozoic of California: *Geology*, v. 19, p. 784-786.
- Goldfarb, R.J., Hart, C., Davis, G., and Groves, D., 2007, East Asian gold: Deciphering the anomaly of Phanerozoic gold in Precambrian cratons: *Economic Geology*, v. 102, p. 341-345.
- Goldfarb, R.J., Hart, C., and Marsh, E.E., 2008, Orogenic gold and evolution of the cordilleran orogen, *in* Spencer, J.E., and Titley, S.R., eds., *Ores and orogenesis: Circum-Pacific tectonics, geologic evolution, and ore deposits*: Arizona Geological Society Digest 22, p. 311-323.
- Haugerud, R.A., and Kunk, M.J., 1988, ArAr*: A computer program for reduction of $^{40}\text{Ar}/^{39}\text{Ar}$ data: U.S. Geological Survey Open-File Report 88-0261, 67 p.
- Horsman, E., Tikoff, B., and Czeck, D., 2008, Rheological implications of heterogeneous deformation at multiple scales in the Late Cretaceous Sierra Nevada, California: *Geological Society of America Bulletin*, v. 120, p. 238-255.
- Irwin, W.P., 2003, Correlation of the Klamath Mountains and Sierra Nevada: Sheet 1 – Map showing accreted terranes and plutons of the Klamath Mountains and Sierra Nevada; Sheet 2 – successive accretionary episodes of the Klamath Mountains and northern part of the Sierra Nevada: U.S. Geological Survey Open-File Report 02-490, 2 sheets, scale 1:1,000,000.
- Irwin, W.P., and Wooden, J.L., 2001, Map showing plutons and accreted terranes of the Sierra Nevada, California, with tabulation of U/Pb isotopic ages: U.S. Geological Survey Open-File Report 2001-229, scale 1:100,000.
- Johnston, W.D., Jr., 1940, The gold quartz veins of Grass Valley, California: U.S. Geological Survey Special Paper 194, 101 p.
- Kirk, J., Ruiz, J., Chesley, J., Walshe, J., and England, G., 2002, A major Archean, gold- and crust-forming event in the Kaapval craton, South Africa: *Science*, v. 297, p. 1856-1858.
- Kistler, R.W., Dodge, F.C.W., and Silberman, M.L., 1983, Isotopic studies of mariposite-bearing rocks from south-central Mother Lode, California: *California Geology*, p. 201-203.
- Knopf, A., 1929, The Mother Lode system of California: U.S. Geological Survey Professional Paper 157, 88 p.
- Kuhl, T.O., 1989, Geology of the Royal - Mountain King Mine, Hodson District, Calaveras County, California: Meridian Gold Company, Copperopolis, California: Las Vegas, Nevada, SME Annual Meeting.
- Kunk, M.J., and Burton, W.C., 1999, $^{40}\text{Ar}/^{39}\text{Ar}$ age-spectrum data for amphibole, muscovite, biotite, and K-feldspar samples from metamorphic rocks in the Blue Ridge anticlinorium, northern Virginia: U.S. Geological Survey Open-File Report, 99-0552, 110 p.
- Landefeld, L.A., 1988, The geology of the Mother Lode gold belt, Sierra Nevada Foothills metamorphic belt, California, *in* Kusvarsanyi, A., and Grant, S. K., eds, *North American Conference on tectonic control of ore deposits and vertical and horizontal extent of ore systems*: University of Missouri-Rolla Special Publication, p. 47-56.
- Landefeld, L.A., and Snow, G.G., eds., 1990, Guidebook to Yosemite and the Mother Lode gold belt: Geology, tectonics, and the evolution of hydrothermal fluids in the Sierra Nevada of California, with articles on operating mines in the Mother Lode, land use and permitting, history and natural history of the Sierra Nevada: Pacific Section, American Association of Petroleum Geologists, Guidebook 68, 200 p.
- Marshall, B., and Taylor, B.E., 1980, Origin of hydrothermal fluids responsible for gold deposition, Alleghany District, Sierra County, California: *Geological Society of America Abstracts with Programs*, v. 12, p. 118.
- McAllister, C.A., 1990, The Pine Tree and Josephine Mines of the southern Mother Lode, Mariposa County, California: mining history, geology, and the fluid inclusion study applied to gold exploration: M.S. Thesis, California State University, Fresno, 265 p.
- McDougall, I., and Harrison, T.M., 1999, *Geochronology and thermochronology by the $^{40}\text{Ar}/^{39}\text{Ar}$ Method*: Oxford, U.K., Oxford University Press, 269 p.
- Miller, R.B., and Paterson, S.R., 1991, Geology and tectonic evolution of the Bear Mountain fault zone, Foothills terrane, central Sierra Nevada, California: *Tectonics*, v. 10, p. 995-1006.
- Montigny, R., 1989, The conventional potassium-argon method, *in* Roth, E., and Poty, B., eds., *Nuclear methods of dating*: Kluwer Academic Publishing, p. 295-321.
- Morelli, R.M., Creaser, R.A., Selby, D., Kontak, D., and Horne, R.J., 2005, Rhenium-osmium geochronology of arsenopyrite in Meguma Group gold deposits, Meguma terrane, Nova Scotia, Canada: Evidence of multiple gold-mineralizing events: *Economic Geology*, v. 100, p. 1229-1242.
- Neidig, S.D., 2001, A report on the Jamestown Mine, Harvard-Crystalline open-pit, Tuolumne County, California: The geology and development history of a mesothermal lode gold deposit: A project report created for the USGS with geographic and geologic data themes on an accompanying media disk (CD-ROM UNR_USGS_jmtwn_PR), 19 p.
- Poole, F.G., Stewart, J.H., Palmer, A.R., Sandberg, C.A., Madrid, R.J., Ross, R.J., Hintze, L.F., Miller, M.M., and Wrucke, C.T., 1993, Latest Precambrian to latest Devonian time – development of a continental margin, *in* Burchfiel, B.C., Lipman, P.W., and Zoback, M.L., eds., *The Cordilleran orogen: Conterminous U.S.*: Geological Society of America, *The Geology of North America*, v. G-3, p. 9-56.
- Saleeby, J.B., 1990, Geochronological and tectonostratigraphic framework of Sierran-Klamath ophiolitic assemblages: *Geological Society of America Special Paper* 255, p. 93-114.
- Saleeby, J., Ducea, M., and Clemens-Knott, D., 2003, Production and loss of high density batholithic root, southern Sierra Nevada, California: *Tectonics*, v. 22, p. 3-1 to 3-24.
- Saleeby, J.B., Geary, E.E., Paterson, S.P., and Tobisch, O.T., 1989, Isotopic systematics of Pb/U (zircon) and $^{40}\text{Ar}/^{39}\text{Ar}$ (biotite-hornblende) from rocks of the central Foothills terrane, Sierra Nevada, California: *Geological Society of America Bulletin*, v. 101, p. 1481-1492.
- Selby, D., Creaser, R.A., Hart, C.J.R., Rombach, C.S., Thompson, J.F.H., Smith, M.S., Bakke, A.A., and Goldfarb, R.J., 2002, Absolute timing of sulfide and gold mineralization: A comparison of Re-Os molybdenite and Ar-Ar mica methods from the Tintina gold belt, Alaska: *Geology*, v. 30, p. 791-794.
- Sharp, W.D., 1988, Pre-Cretaceous crustal evolution of the Sierra Nevada region, *in* Ernst, W.G., ed., *Metamorphism and crustal evolution of the western United States*: Englewood Cliffs, New Jersey, Prentice-Hall, p. 824-864.
- Sibson, R., and Elliot, J., 1993, Field trip to the southern Mother Lode: Field trip guide, Fish Camp, California, June 6-10, 1993, 21 p.
- Snow, C.A., and Scherer, H., 2006, Terranes of western Sierra Nevada Foothills metamorphic belt: A critical review: *International Geology Review*, v. 48, p. 46-62.
- Snow, C.A., Bird, D.K., Metcalf, J., and McWilliams, M., 2008, Chronology of gold mineralization in the Sierra Nevada Foothills from $^{40}\text{Ar}/^{39}\text{Ar}$ dating of mariposite: *International Geology Review*, v. 50, p. 503-518.

- Standlee, L.A., 1978, Middle Paleozoic ophiolites in the Melones fault zone, northern Sierra Nevada, California: Geological Society of America Abstracts and Programs, v. 10, p. 148.
- Staudacher, T., Jessberger, E.K., Dörflinger, D., and Kiko, J., 1978, A refined ultrahigh-vacuum furnace for rare gas analysis: Journal of Physics E: Scientific Instruments, v. 11, p. 781-784.
- Steiger, R.H., and Jäger, E., 1977, Subcommittee on geochronology; convention on the use of decay constants in geo- and cosmochronology: Earth and Planetary Science Letters, v. 36, p. 359-362.
- Tobisch, O.T., Paterson, S.R., Saleeby, J.B., and Geary, E.E., 1989, Nature and timing of deformation in the Foothills terrane, central Sierra Nevada, California—Its bearing on orogenesis: Geological Society of America Bulletin, v. 101, p. 401-413.
- Tobisch, O.T., Saleeby, J.B., Renne, P.R., McNulty, B.A., and Tong, W., 1995, Variations in deformation fields during development of a large-volume magmatic arc, central Sierra Nevada, California: Geological Society of America Bulletin, v. 107, p. 1043-1058.
- Umhoefer, P.J., 2003, A model for the North America Cordillera in the early Cretaceous: Tectonic escape related to arc collision of the Guerrero terrane and a change in North America plate motion, *in* Johnson, S.E., Paterson, S.R., Fletcher, J.M., Girty, G.H., Kimbrough, D.L., and Martin-Barajas, A., eds., Tectonic evolution of northwestern Mexico and the southwestern USA: Boulder, Colorado, Geological Society of America Special Paper 374, p. 117-134.
- Weir, R.H. Jr., 1986, Mineralogic, fluid inclusion, and stable isotope studies of several gold mines in the Mother Lode, Tuolumne and Mariposa Counties, California: M.S. Thesis, University Park, Pennsylvania State University, 98 p.
- Weir, R.H., Jr., and Kerrick, D.M., 1987, Mineralogic, fluid inclusion, and stable isotope studies of several mines in the Mother Lode, Tuolumne and Mariposa Counties, California: Economic Geology, v. 82, p. 328-344.
- York, D., 1969, Least squares fitting of a straight line with correlated errors: Earth and Planetary Science Letters, v. 5, p. 320-324.

Appendix: Table A1. Summary of new argon-isotope analyses.

	TEMP (°C)	% ³⁹ Ar (of total)	Radiogenic Yield (%)	³⁹ Ar _K (Moles x 10 ⁻¹²)	⁴⁰ Ar*/ ³⁹ Ar _K ±.5%	Apparent K/Ca	Apparent K/Cl	Apparent Age (Ma)	Error (Ma)
MARIPOSITE									
51KD47 Quartz Hill				<i>J=.011465</i>	<i>±.5%</i>	<i>.0193 g</i>			
A	500	0.6	12.6	0.053559	2.031	64.0	54	41.53	3.48
B	600	2.5	83.2	0.229654	5.717	110.9	280	114.52	0.52
C	700	10.3	98.5	0.960196	6.482	143.7	1900	129.32	0.09
D	750	15.0	99.6	1.401965	6.522	278.3	6004	130.09	0.13
E	800	22.1	99.7	2.068966	6.519	330.9	10568	130.04	0.09
F	825	16.0	99.6	1.497077	6.479	342.8	16749	129.26	0.13
G	850	13.5	99.7	1.266334	6.461	404.1	23554	128.91	0.12
H	875	9.5	99.7	0.886367	6.440	395.2	7888	128.51	0.11
I	900	4.4	99.2	0.410592	6.404	410.8	3336	127.81	0.20
J	925	2.4	98.9	0.227370	6.414	315.9	1477	128.01	0.17
K	950	1.2	98.1	0.111593	6.459	244.7	583	128.88	0.38
L	1000	1.1	97.6	0.103789	6.475	247.6	386	129.17	0.57
M	1050	0.5	95.9	0.048431	6.436	122.9	204	128.44	1.14
N	1100	0.6	98.3	0.053489	6.570	133.0	295	131.02	0.91
O	1250	0.2	79.9	0.022444	6.415	32.7	2	128.03	3.14
P	1450	0.1	80	0.009932	6.882	35.8	37	137.00	6.90
Total Gas			98.5	9.351800	6.440	312.7	10255	128.51	
		63.39 % gas released on plateau in steps			700	825 Average age		129.67	0.70
53KD47 Alameda				<i>J=.011532</i>	<i>±.5%</i>	<i>.0208 g</i>			
A	500	0.5	17	0.050895	1.910	74.2	25	39.31	2.59
B	600	1.5	80.1	0.169949	5.354	111.7	106	108.08	0.62
C	700	4.7	98	0.518554	6.571	136.0	584	131.76	0.20
D	750	8.4	99.6	0.924634	6.638	262.1	1433	133.06	0.18
E	800	16.6	99.7	1.824145	6.577	345.6	5593	131.88	0.22
F	850	26.8	99.9	2.947798	6.564	389.5	25747	131.64	0.12
G	900	22.4	99.9	2.468982	6.498	440.4	118246	130.35	0.17
H	925	7.3	99.6	0.804514	6.478	371.4	3853	129.96	0.16
I	950	4.3	99.6	0.470991	6.543	321.5	2470	131.22	0.21
J	975	3.0	99.4	0.329177	6.502	345.5	1617	130.44	0.54
K	1000	1.5	99.2	0.166950	6.513	273.2	780	130.65	0.42
L	1025	0.9	98.3	0.101652	6.548	225.7	429	131.32	0.65
M	1050	0.5	99.8	0.059519	6.647	171.1	456	133.24	1.16
N	1100	1.2	99	0.130507	6.580	174.1	938	131.95	0.52
O	1150	0.3	97.5	0.029728	6.763	84.7	98	135.48	2.30
P	1200	0.1	85.6	0.007902	7.599	22.0	1	151.54	9.18
Q	1250	0.0	92.1	0.003771	8.228	7.4	27	163.53	17.48
Total Gas			99	11.009700	6.510	351.5	34952	130.59	
		No Plateau							
55KD47 McAlpine				<i>J=.011651</i>	<i>±.5%</i>	<i>.0199 g</i>			
A	500	5.8	79	0.526158	5.409	134.9	313	110.25	0.26
B	600	4.5	98.7	0.407633	6.141	137.9	2410	124.67	0.21
C	700	30.4	99.9	2.750241	6.069	203.4	15005	123.24	0.09
D	750	28.3	99.8	2.560452	6.157	255.1	13842	124.98	0.19
E	800	20.5	99.7	1.856336	6.082	288.7	28331	123.51	0.16
F	825	6.7	99.2	0.606536	6.050	281.2	4205	122.87	0.18
G	850	2.0	98.2	0.183861	6.009	251.5	1077	122.08	0.34
H	875	0.6	96.4	0.054141	6.025	167.8	368	122.38	0.83
I	900	0.2	92	0.021156	5.922	70.6	138	120.37	1.46
J	950	0.2	90.2	0.017925	6.062	42.8	83	123.12	4.02
K	1000	0.2	90.7	0.015392	6.173	47.7	60	125.30	2.45
L	1100	0.3	87.2	0.029446	5.983	44.8	91	121.57	1.69
M	1250	0.0	45.8	0.004343	6.731	7.8	0	136.19	7.50
Total Gas			98.3	9.033600	6.058	233.1	14747	123.05	
		No Plateau							

Appendix: Table A1 continued. Summary of new argon-isotope analyses.

	TEMP (°C)	% ³⁹ Ar (of total)	Radiogenic Yield (%)	³⁹ Ar _K (Moles × 10 ⁻¹²)	⁴⁰ Ar*/ ³⁹ Ar _K	Apparent K/Ca	Apparent K/Cl	Apparent Age (Ma)	Error (Ma)
57KD47 Carson Hill Pit				<i>J=0.11528</i>	<i>±5%</i>	<i>.0199 g</i>			
A	500	0.7	29.8	0.082099	5.095	58.8	31	102.97	1.73
B	600	1.0	90.3	0.125857	6.328	120.6	463	127.03	0.34
C	700	5.1	98.8	0.615067	6.534	257.9	1277	131.00	0.14
D	750	7.3	99	0.878991	6.666	398.0	2708	133.56	0.15
E	800	10.6	99.4	1.273277	6.665	472.6	5414	133.55	0.16
F	825	10.5	99.6	1.262729	6.772	508.3	7759	135.60	0.17
G	850	10.4	99.7	1.254614	6.752	577.0	14855	135.23	0.12
H	875	7.2	99.6	0.865667	6.710	665.8	9520	134.40	0.07
I	900	5.7	99.5	0.680377	6.766	628.9	4621	135.49	0.15
J	925	4.4	99.5	0.528372	6.788	774.2	2746	135.92	0.14
K	950	3.8	99.4	0.457769	6.768	582.2	1796	135.53	0.23
L	1000	6.6	99.5	0.798964	6.771	736.7	4102	135.59	0.11
M	1050	9.1	99.5	1.092440	6.761	783.6	6627	135.39	0.20
N	1100	9.8	99.5	1.175307	6.820	707.1	6081	136.53	0.18
O	1240	5.6	99.2	0.673177	6.740	576.3	72	134.99	0.15
P	1450	1.8	98.9	0.216105	6.859	357.3	2027	137.29	0.34
Q	1650	0.4	95.5	0.045016	6.812	159.5	486	136.38	0.82
Total Gas			98.8	12.025800	6.722	575.7	5853	134.64	
		No Plateau							
59KD47 Oxford Mine				<i>J=0.1151</i>	<i>±5%</i>	<i>.0193 g</i>			
A	500	0.1	2.7	0.007848	0.958	21.0	36	19.78	7.33
B	600	2.7	59.7	0.265930	5.304	94.2	254	106.91	0.40
C	700	10.1	98.3	1.005825	5.952	127.0	2930	119.54	0.05
D	750	14.4	99.2	1.432183	5.926	303.4	7577	119.03	0.15
E	800	20.2	99.3	2.014929	5.896	342.8	12288	118.44	0.12
F	825	15.2	99.4	1.512767	5.848	364.8	116526	117.52	0.18
G	850	11.6	99.4	1.156980	5.832	399.6	161873	117.21	0.13
H	875	7.4	99.5	0.734529	5.815	444.8	15443	116.87	0.13
I	900	4.4	99.3	0.437034	5.793	449.6	5530	116.46	0.19
J	925	2.7	99.5	0.274110	5.833	375.5	2788	117.23	0.26
K	950	2.0	99.2	0.200168	5.814	321.7	1758	116.85	0.20
L	1000	2.5	99.2	0.251903	5.816	325.0	1916	116.88	0.22
M	1050	2.4	99	0.240251	5.833	361.6	1501	117.22	0.28
N	1100	3.0	99.2	0.297054	5.862	365.2	2474	117.79	0.20
O	1250	1.1	93	0.110643	5.915	145.7	11	118.81	0.40
P	1450	0.3	90	0.033255	5.935	50.3	131	119.20	1.40
Total Gas			98	9.975400	5.853	328.6	41968	117.62	
		No Plateau							
61KD47 Pine Tree/Josephine				<i>J=0.11625</i>	<i>±5%</i>	<i>.0156 g</i>			
A	500	0.4	8	0.032179	1.707	45.9	27	35.45	3.81
B	600	1.9	74.7	0.145278	5.025	95.6	134	102.42	0.70
C	700	7.8	96.4	0.592181	5.722	127.2	1334	116.17	0.23
D	750	14.4	98.9	1.092840	5.734	216.1	3006	116.41	0.19
E	800	21.1	99.2	1.603061	5.804	313.3	5191	117.80	0.15
F	825	16.5	99.2	1.251766	5.738	341.0	7986	116.49	0.19
G	850	13.2	99.4	0.999788	5.718	400.1	5937	116.09	0.12
H	875	8.1	99.3	0.613576	5.661	421.3	5653	114.97	0.17
I	900	4.5	99	0.341444	5.722	352.1	2103	116.18	0.21
J	925	2.8	99.1	0.213475	5.713	300.9	1171	115.99	0.34
K	950	2.1	98.9	0.162598	5.696	291.5	909	115.67	0.38
L	1000	2.5	99.1	0.189274	5.754	294.0	707	116.81	0.34
M	1050	1.5	98.1	0.116090	5.729	217.0	500	116.32	0.51
N	1100	2.1	98.9	0.160086	5.790	203.7	882	117.51	0.42
O	1250	0.6	92.7	0.046953	5.941	49.6	5	120.48	1.51
P	1450	0.3	88.8	0.024754	5.824	43.8	95	118.18	2.09
Total Gas			98	7.585300	5.711	298.4	4386	115.96	
		No Plateau							

Appendix: Table A1 continued. Summary of new argon-isotope analyses.

	TEMP (°C)	% ³⁹ Ar (of total)	Radiogenic Yield (%)	³⁹ Ar _K (Moles x 10 ⁻¹²)	⁴⁰ Ar/ ³⁹ Ar _K	Apparent K/Ca	Apparent K/Cl	Apparent Age (Ma)	Error (Ma)
63KD47 Quartz Hill, Placerville				<i>J=0.11574</i>	<i>±.5%</i>	<i>.0191 g</i>			
A	500	0.5	20.3	0.051934	2.369	41.0	41	48.79	1.72
B	600	0.7	85.3	0.082049	6.101	90.6	214	123.09	0.31
C	700	3.2	98	0.358427	6.280	219.2	1204	126.57	0.25
D	750	4.7	99.4	0.533795	6.215	413.6	2500	125.31	0.18
E	800	8.8	99.7	0.994949	6.207	706.0	7440	125.15	0.11
F	825	8.9	99.9	1.010998	6.180	673.7	190572	124.63	0.06
G	850	10.8	99.8	1.219597	6.173	645.1	0	124.50	0.08
H	875	11.6	99.8	1.310285	6.122	812.0	0	123.50	0.18
I	900	10.5	99.9	1.181926	6.157	1008.6	0	124.19	0.13
J	925	8.9	99.8	1.004663	6.114	1094.0	0	123.34	0.15
K	950	6.5	99.7	0.736985	6.119	1073.4	23801	123.44	0.18
L	1000	7.8	99.8	0.881384	6.142	1754.9	21138	123.90	0.15
M	1050	5.6	99.5	0.632397	6.127	959.8	4847	123.60	0.18
N	1100	4.9	99.6	0.551112	6.137	869.0	3570	123.79	0.17
O	1250	5.8	98.7	0.655077	6.177	479.4	59	124.58	0.21
P	1450	0.8	97.2	0.095003	7.232	57.3	333	145.01	0.74
Total Gas			99.1	11.300600	6.150	847.5	21515	124.05	
			No Plateau						
65KD47 Harvard Pit				<i>J=0.1159</i>	<i>±.5%</i>	<i>.0191 g</i>			
A	600	1.4	59.5	0.133839	4.915	67.0	26	99.95	0.85
B	700	3.9	96.8	0.365053	6.304	76.7	541	127.21	0.24
C	750	2.4	98.7	0.218302	6.445	147.8	925	129.96	0.26
D	800	14.3	99.5	1.328377	6.528	288.1	2773	131.58	0.18
E	825	11.5	99.5	1.068447	6.484	527.4	5433	130.73	0.07
F	850	12.1	99.8	1.124216	6.467	585.4	7725	130.39	0.15
G	875	11.7	99.8	1.089394	6.425	629.3	10800	129.57	0.22
H	900	9.8	99.9	0.906582	6.462	719.8	6230	130.29	0.11
I	925	7.5	99.8	0.698117	6.433	666.4	5175	129.73	0.17
J	950	5.2	99.7	0.477681	6.449	669.1	3135	130.03	0.19
K	1000	5.9	99.6	0.550741	6.436	739.6	2558	129.79	0.21
L	1050	5.1	99.6	0.474169	6.419	804.5	2128	129.46	0.18
M	1100	5.6	99.6	0.518799	6.451	736.0	3018	130.09	0.17
N	1250	2.8	99.2	0.258413	6.470	296.5	31	130.44	0.27
O	1450	0.7	96.8	0.060898	6.528	154.4	336	131.57	0.94
Total Gas			98.9	9.273000	6.435	544.9	4865	129.76	
			50.85 % gas released on plateau in steps						
					875	1100 Average age	129.94	0.70	
67KD47 Jack Adit				<i>J=0.11622</i>	<i>±.5%</i>	<i>.0204 g</i>			
A	500	0.6	35.9	0.077406	5.094	26.6	83	103.76	1.33
B	600	0.2	89.7	0.019280	6.030	29.3	493	122.20	2.15
C	700	1.4	96.8	0.165375	6.247	5.1	923	126.43	0.34
D	750	3.0	98.8	0.354973	6.407	2.2	1712	129.56	0.23
E	800	5.8	99.4	0.692695	6.435	5.2	3818	130.10	0.09
F	825	3.7	99.5	0.442403	6.453	258.2	7467	130.47	0.16
G	850	5.3	99.6	0.633817	6.416	342.7	48343	129.73	0.25
H	875	4.9	99.4	0.583883	6.418	351.8	44288	129.78	0.07
I	900	6.2	99.5	0.742104	6.484	466.3	25486	131.07	0.17
J	925	6.8	99.4	0.809261	6.490	744.1	35762	131.18	0.17
K	950	6.9	99.4	0.820108	6.513	1069.5	19629	131.63	0.20
L	1000	13.4	99.5	1.600407	6.554	1570.7	92236	132.43	0.17
M	1050	15.5	99.6	1.845020	6.582	2569.7	0	132.97	0.09
N	1100	12.0	99.6	1.428566	6.540	2158.2	23247	132.17	0.08
O	1250	13.0	99.4	1.551374	6.502	2382.0	156	131.41	0.15
P	1450	1.4	98.6	0.170875	6.653	318.9	561	134.36	0.39
Total Gas			99	11.937500	6.496	1378.7	25829	131.30	
			No Plateau						

Appendix: Table A1 continued. Summary of new argon-isotope analyses.

	TEMP (°C)	% ³⁹ Ar (of total)	Radiogenic Yield (%)	³⁹ Ar _K (Moles x 10 ⁻¹²)	⁴⁰ Ar*/ ³⁹ Ar _K	Apparent K/Ca	Apparent K/Cl	Apparent Age (Ma)	Error (Ma)
69KD47 16:1				J= .011558	±.5%	.0199 g			
A	500	0.3	17.8	0.028932	2.352	44.1	74	48.39	1.86
B	600	1.2	85.8	0.121133	6.180	80.4	416	124.46	0.59
C	700	5.5	97.7	0.548520	5.760	118.5	1464	116.27	0.67
D	750	9.3	99.3	0.924002	5.801	196.9	2024	117.07	0.15
E	800	13.3	99.4	1.327663	5.775	264.9	4467	116.55	0.15
F	825	12.9	99.4	1.282197	5.743	361.0	5494	115.93	0.09
G	850	12.0	99.5	1.191169	5.727	459.1	7411	115.62	0.16
H	875	11.0	99.6	1.092605	5.704	475.1	8011	115.17	0.13
I	900	8.7	99.6	0.862535	5.681	527.1	7156	114.72	0.13
J	925	6.5	99.6	0.643646	5.697	537.8	3286	115.05	0.15
K	950	4.3	99.4	0.427697	5.740	525.7	1694	115.87	0.17
L	1000	4.4	99.4	0.434633	5.710	543.1	1609	115.29	0.18
M	1050	3.1	99.2	0.310216	5.700	519.1	999	115.09	0.18
N	1100	4.0	99.4	0.393443	5.725	507.5	1588	115.59	0.17
O	1250	3.1	98.8	0.312048	5.787	157.4	32	116.79	0.21
P	1450	0.5	93.8	0.046737	5.867	86.9	166	118.36	1.07
Total Gas			98.9	9.947200	5.733	383.4	4418	115.74	
			No Plateau						
WHITE MICA									
71KD47 Confidence				J= .011702	±.5%	.0212 g			
A	500	0.2	10.1	0.021759	1.913	29.6	19	39.94	2.37
B	600	1.1	71.8	0.121516	5.649	54.4	80	115.48	0.77
C	700	3.7	96.2	0.403591	6.317	71.3	764	128.66	0.19
D	750	4.4	97.7	0.476954	6.525	83.0	1289	132.73	0.15
E	800	5.8	97.9	0.631707	6.528	104.7	1423	132.81	0.23
F	850	7.2	97.4	0.783056	6.407	113.0	2004	130.42	0.24
G	900	10.1	97.2	1.102862	6.312	124.6	3396	128.57	0.16
H	925	7.5	97.1	0.818447	6.287	148.0	4996	128.06	0.17
I	950	10.9	97.3	1.188224	6.290	156.1	5958	128.13	0.19
J	975	9.6	97.3	1.048425	6.285	177.9	5848	128.03	0.12
K	1000	8.3	97.5	0.905883	6.301	177.5	6545	128.34	0.15
L	1025	8.5	97.4	0.925565	6.284	180.6	6002	128.01	0.18
M	1050	6.5	97.3	0.707144	6.294	157.3	6231	128.19	0.21
N	1100	9.5	97.1	1.042421	6.228	152.4	3950	126.90	0.10
O	1150	4.7	97.2	0.518708	6.267	104.0	1084	127.68	0.22
P	1200	1.1	94.6	0.117809	6.087	49.0	10	124.13	0.49
Q	1250	0.5	94.5	0.049966	5.744	17.5	284	117.35	0.90
R	1450	0.7	92.7	0.077137	5.542	24.9	166	113.35	0.69
Total Gas			96.8	10.941200	6.293	139.0	4117	128.18	
			61.21 % gas released on plateau in steps		900	1050 Average age		128.18	0.69